ELECTRON SPIN RESONANCE STUDY OF FREE RADICAL FORMATION IN IRRADIATED ZINC ACETATE DIHYDRATE

JOSEPH LOUIS VALENTI

ELECTRON SPIN RESONANCE STUDY OF FREE RADICAL FORMATION IN IRRADIATED ZINC ACETATE DIHYDRATE

by

Joseph Louis Valenti
Lieutenant, United States Coast Guard
B.S., Coast Guard Academy, 1962

Submitted in partial fulfillment of the
requirements for the degree of

MASTER OF SCIENCE IN PHYSICS

from the

NAVAL POSTGRADUATE SCHOOL
June 1967

ABSTRACT

An electron spin resonance analysis of irradiated zinc acetate dihydrate, $Zn(CH_3COO)_2 2H_2O$ has been made. The methyl radical, $\cdot CH_3$ has been identified in the spectra of polycrystalline samples irradiated at 77°K and examined at 103°K. The proton hyperfine splitting was determined to be -61.7 ± 1.0 Mc. The conversion of $\cdot CH_3$ into a radical tentatively identified as $\cdot CH_2CO_2^-$ was observed. The conversion is believed to occur too rapidly to be observed in spectra of samples irradiated at 300°K. The X, Y, Z components of the hyperfine interaction tensors of the α_1 and α_2 protons of $\cdot CH_2CO_2^-$ have been tentatively determined to be :-92 ± 5, -64 ± 5, -24 ± 5; and -91 ± 5, -60 ± 5, -38 ± 5Mc respectively. The X, Y, Z orthogonal axis system was formulated with the Z axis along the CH_1 bond and the X axis perpendicular to Z and in the plane of the CH and CC bonds. The tensor elements were calculated from first order perturbation theory although second order lines of significant intensity were observed. The H_1CH_2 angle was found to be 123.5° ± 5°. The limits of error on tensor components and the bond angle were estimated. Orientations of the CH bonds were found to be rotated 90° about the b axis from the location implied by the crystal structure.

TABLE OF CONTENTS

LIST OF TABLES

LIST OF ILLUSTRATIONS

1. Introduction

Extensive studies of the electron spin resonance spectra of the free radicals present in various liquids and solid matrices have been made (4), (12), (23). In the liquid phase, rapid tumbling of the molecules has the effect of averaging out the anisotropies of the hyperfine coupling tensor and the electron spectroscopic splitting tensor (22), (24). Because of this time averaging effect the analysis of liquid phase electron spin resonance spectra is, in principle, quite straightforward (5). In the solid state most of the analyses have been carried out using single crystal hosts thus positioning the radicals at well defined orientations in the crystal lattice (23). However, spectra of free radicals trapped in polycrystalline samples are in general most difficult to interpret since, because of the anisotropy, the resonance lines are somewhat broadened and tend to obscure the weaker resonance signals (7).

An ideal way to attack the problem of radical identification in polycrystalline lattices would be: (a) formulate a model for each radical whose presence is suspected; (b) determine the associated tensors; (c) calculate the theoretical line shapes; and (d) compare the experimental spectra with that calculated to determine whether a proper identification of the paramagnetic species has been made.

The use of computers to calculate the theoretical spectra in the case of amorphous or polycrystalline samples has been the subject of several papers (3), (8), (18), (19). Such a computation usually involves a spatial average over different magnetic site orientations. The general treatment of the problem is quite detailed and arrival at a solution is a time consuming process even for a computer.

The purposes of this investigation were: (a) to formulate a more efficient means in terms of required computer time of predicting line shapes for free radicals trapped in polyoriented hosts; (b) to undertake the study of radiation damage in a polycrystalline sample; and (c) to attempt to grow single crystals of the material and perform a spectral interpretation if an initial polycrystalline study showed promise, or attempt to extract data using the polycrystalline spectral prediction program if either the difficulty of obtaining single crystals or the existence of many inequivalent magnetic sites in the unit cell made a single crystal analysis impractical.

An initial study of irradiated sodium acetate trihydrate was abruptly terminated by the untimely publication of its analysis (14). In hopes of finding another material which, when irradiated, might yield analogous results, a routine investigation of free radical formation in irradiated acetates was undertaken. As a result of this, zinc acetate dihydrate, $Zn(CH_3COO)_2 \cdot 2H_2O$, was selected to be studied.

A literature search revealed that a previous study of irradiated zinc acetate dihydrate resulted in the identification of the methyl radical (15). An initial study of polycrystalline samples irradiated at 77°K and examined at 103°K confirmed the presence of the methyl radical. However, the study further revealed: (a) that the methyl radical undergoes an apparent conversion into a new species; (b) that spectra identical to those observed after conversion result when samples are irradiated and observed at room temperature, implying that conversion occurs rapidly under these conditions; and (c) that the centerline of the spectrum of samples irradiated at 300°K seems to split as the sample temperature is lowered. In view of these observations it was decided that further study of radiation damage in zinc acetate dihydrate was justified.

Thus, the investigation was pursued in hopes that: (a) an identification of the species present after conversion could be made; (b) the coupling constants, orientation in the crystal and bond angles of the radical could be determined; and (c) that a suitable explanation for the behavior with temperature variation could be found.

2. The Spin Hamiltonian

A general spin Hamiltonian which describes the interaction of nuclei and an electron in an external magnetic field $\vec{H}$ for the case of quenched orbital angular momentum can be written as

$$\mathcal{H} = \beta \vec{H} \cdot \vec{\vec{g}} \cdot \vec{S} - \sum_i \gamma_i \hbar \vec{H} \cdot \vec{I}_i + \sum_i \gamma_i \hbar \vec{S} \cdot \vec{\vec{A}}_i \cdot \vec{I}_i \qquad (2), (28)$$

The first term represents the Zeeman energy, the energy of interaction of the electron spin moment with the external magnetic field. β is the Bohr magneton; $\vec{S}$ is the electronic spin; and $\vec{\vec{g}}$ is the spectroscopic splitting tensor. The second term is the summation of the Zeeman energy of the nuclei where $\vec{I}_i$ is the spin of the ith nucleus and γ_i is the gyromagnetic ratio of the ith nucleus. The third term represents the summation of the energy of the hyperfine interaction between the electronic spin $\vec{S}$ and the spin of the ith nucleus $\vec{I}_i$. $\vec{\vec{A}}_i$ is the hyperfine interaction tensor.

The g tensor is anisotropic when the electron possesses both spin and angular momentum (6). The anisotropy is believed to be caused by spin-orbit interaction between the zeroth state and excited states of the radical (21). In molecules with negligible spin-orbit interaction the hyperfine interaction tensor's anisotropy is a result of dipole-dipole interaction between $\vec{u}_e$, the magnetic moment of the electron, and $\vec{u}_m$, the magnetic moment of the ith nucleus (1), (7).

Since to first order the nuclear Zeeman energy may be neglected it will not be considered in the calculations which follow.

3. The Polycrystalline Calculation

3.1 A First Order Approximation to the Spin Hamiltonian

In order to perform the polycrystalline calculation, an expression which is a suitable approximation to first order of the spin Hamiltonian must be developed so that it may be used in performing a spacial average of the existing magnetic sites. This can be accomplished by expressing the $\vec{\vec{g}}$ and $\vec{\vec{A}}_i$ tensors in terms of their principal values and trigonometric functions.

When an external magnetic field $\vec{H}$ is oriented at a polar angle θ and and azimuthal angle ϕ with respect to the principal axis system of the hyperfine interaction tensor of a nucleus, as shown in Figure 1 for an $\propto$ proton, the magnitude of the coupling constant may be expressed to first order as

$$a = (A_{xx}^2 \mathrm{Sin}^2\theta\mathrm{Cos}^2\phi + A_{yy}^2 \mathrm{Sin}^2\theta\mathrm{Sin}^2\phi + A_{zz}^2 \mathrm{Cos}^2\theta)^{\frac{1}{2}} \qquad (2)$$

Since the principal axis systems of the $\vec{\vec{A}}$ and $\vec{\vec{g}}$ tensors are found to coincide in many cases because of symmetry, to first order the g – factor may be expressed as

$$g = (g_{xx}^2 \mathrm{Sin}^2\theta\mathrm{Cos}^2\phi + g_{yy}^2 \mathrm{Sin}^2\theta\mathrm{Sin}^2\phi + g_{zz}^2 \mathrm{Cos}^2\theta)^{\frac{1}{2}} \qquad (17), (28)$$

Combining the above expressions and neglecting the Zeeman energy of the nuclei the transitions to first order are given by the expression

$$h\nu_o = \beta H(g_{xx}^2 \mathrm{Sin}^2\theta\mathrm{Cos}^2\phi + g_{yy}^2 \mathrm{Sin}^2\theta\mathrm{Sin}^2\phi + g_{zz}^2 \mathrm{Cos}^2\theta)^{\frac{1}{2}} + M_I(A_{xx}^2 \mathrm{Sin}^2\theta\mathrm{Cos}^2\phi + A_{yy}^2 \mathrm{Sin}^2\theta\mathrm{Sin}^2\phi + A_{zz}^2 \mathrm{Cos}^2\theta)^{\frac{1}{2}}$$

Here ν_o is the transition frequency and M_I is the projection of the nuclear spin in the direction of the magnetic field due to the electron.

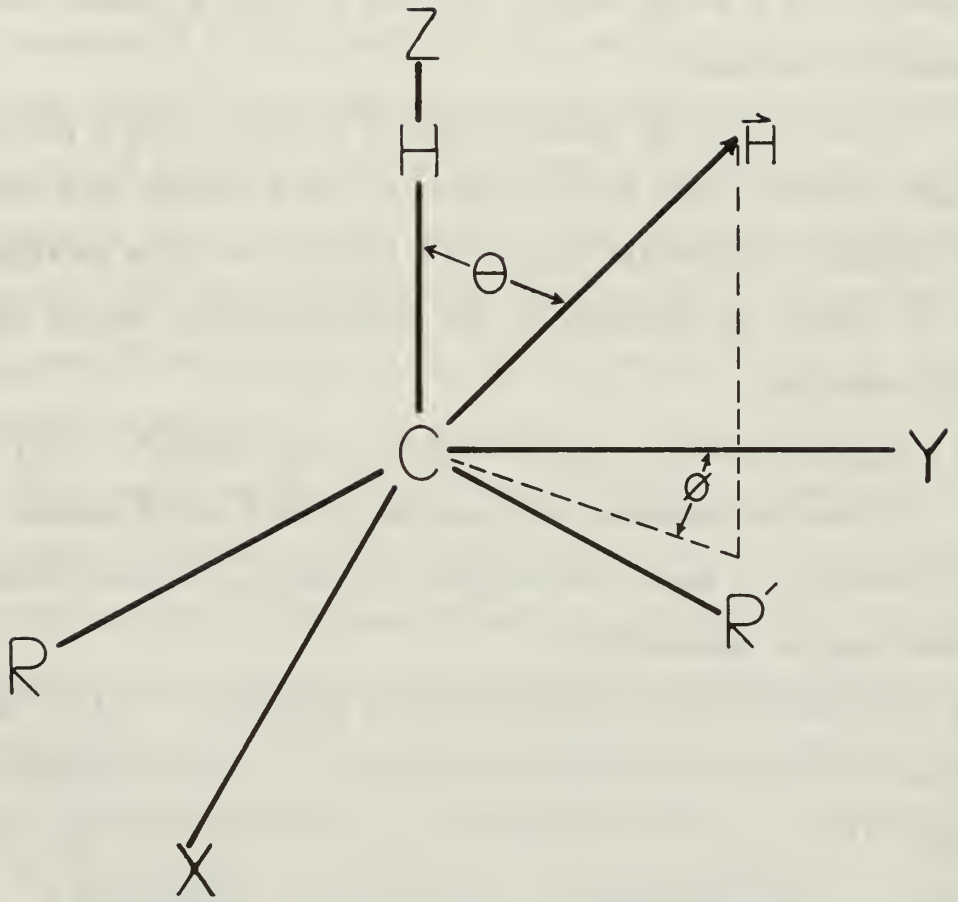

Figure 1. The principal axis coordinate system for the hyperfine interaction tensor of an α proton. $\vec{H}$ represents a magnetic field oriented at a polar angle θ and an azimuthal angle Ø with respect to the axis system.

3.2 The Effect of Polyorientation on Absorption Intensity

In an amorphous or polyoriented sample all orientations of the crystal field principal axes are equally likely (16), (26). Therefore, a means of predicting the effect of having all orientations present for the case of complete anisotropy must be found. The relative number of free radicals N present between the angle θ (measured from the z axis) and the angle $\theta + d\theta$ is given by

$$N = k \sin \theta \, d\theta$$

where k is a constant of proportionality. Inasmuch as power absorption intensity is proportional to the number of radicals present the expected absorption intensity due to the radical population with a value at θ will therefore be proportional to $\sin \theta$.

3.3 The Computer Program

In order to perform the calculation, modifications were made to an existing program which computed spectra for all cases of isotropic $\vec{\vec{g}}$ and $\vec{\vec{A}}$ (29). This program was rewritten so that line positions and intensities were computed for the radicals at a polar angle θ as described in Section 3.2, by incrementing $\emptyset$ at a particular value of θ. The intensities of the lines computed for a particular value of θ were then multiplied by $\sin \theta$ so as to account for the radical population at θ. θ was then incremented and the procedure repeated. The first derivative of the power absorption spectrum of the polycrystalline sample was then constructed by substituting Lorentzian derivative line shapes for all of the computed spectral lines and summing them.

It should be borne in mind that the program was developed with a preconceived realization that it would only be useful for predicting polycrystalline spectra for cases where small anisotropies exist.

3.4 Results

The ESR spectrum of x-rayed polycrystalline ammonium perchlorate, NH_4ClO_4, was produced in the laboratory. Concurrently, a calculation was performed to predict the spectrum using the radical and parameter identifications made by Cole (6). Inasmuch as the anisotropies encountered in ammonium perchlorate are fairly small, it was felt that this comparison would be an excellent means of testing the program. The results are illustrated in Figure 2. Although a basic agreement is apparent, several shoulders present in the experimental spectrum do not occur in the predicted spectrum. In addition to this, there is obviously some disagreement in the intensities of several of the lines. As a further test of the program, an attempt was made to predict the spectrum of the radical FOO· reported by Kasai and Kirshenbaum (13). Figure 3 shows a comparison of the spectrum reported (13) for FOO· from O_2F_2 with that computed. Again, only a basic agreement can be claimed.

At this point it was decided that further development of the polycrystalline spectral prediction program would not be pursued as it was felt that the time remaining for the investigation could best be utilized in the pursuit of an analysis of irradiated zinc acetate dihydrate.

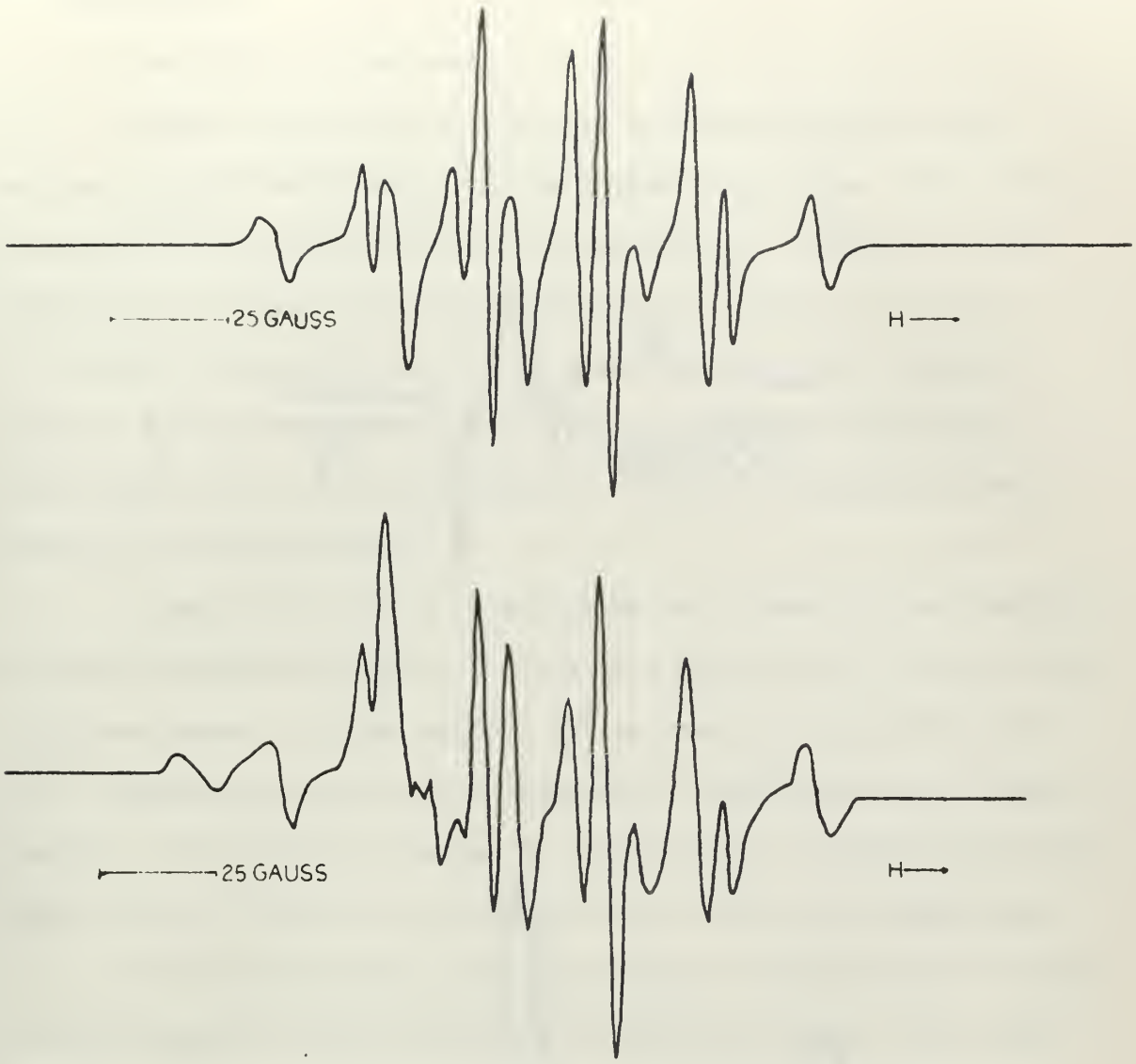

Figure 2. The predicted (top) and observed (bottom) ESR spectrum of irradiated polycrystalline NH_4ClO_4.

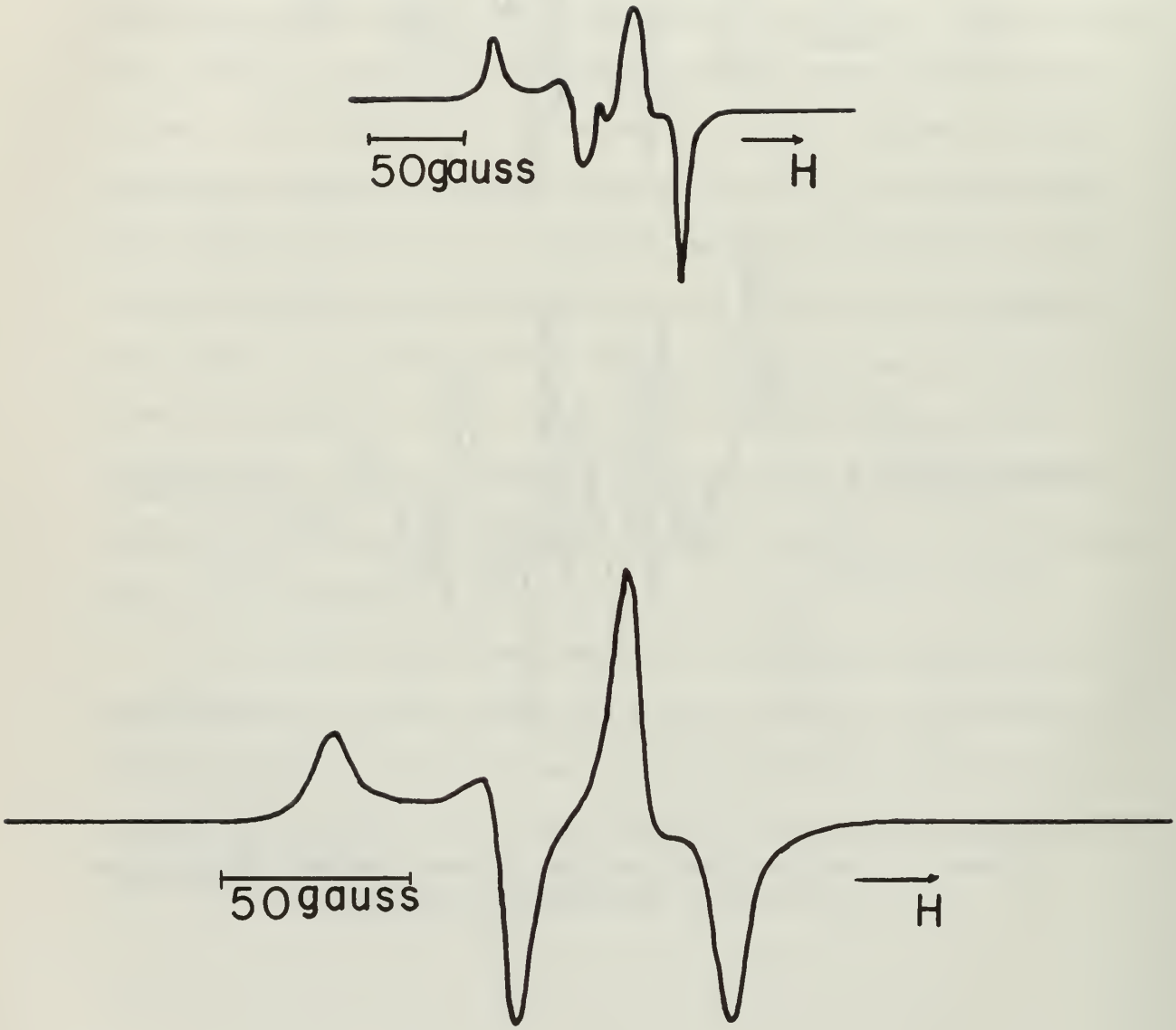

Figure 3. The predicted (top) and observed (bottom, reported by Kasai, et al (13)) ESR spectrum of the FOO· radical from O_2F_2.

4. Experimental

4.1 Materials and Instruments

Single crystals of zinc acetate dihydrate were grown from saturated aqueous solutions by the slow evaporation method. The crystals are monoclinic with space group C2/c. The unit cell contains only four formula units and has dimensions a = 14.50Å, b = 5.32Å, c = 11.02Å, and β = 100°-0'. The zinc atoms lie on a twofold axis (27). Although there are four formula units in the unit cell, only two magnetically inequivalent sites for radical formation should occur because of this particular crystal structure.

Single and polycrystalline samples were exposed to x-irradiation at 50KV and 20ma for from 1 to 2 hours at a distance of 6.5 cm from the molybdinum target. Several polycrystalline samples were irradiated at 77°K. Temperature control was accomplished by immersing samples sealed in 4 mm O.D., 3 mm I.D. quartz tubing in a polystyrene ice bucket filled with liquid nitrogen. All other irradiations were made at room temperature.

The ESR spectrometer used was a Varian V-4502-13 with a Fiedial V-FR 2503 magnetic field regulation and a nine inch magnet, using 100kc modulation, and a conventional reflection type cavity equipped with a Varian variable temperature control unit.

4.2 The Identification of the Crystal Axes in the Macroscopic Crystal

The majority of the crystals grown had macroscopic appearances similar to that illustrated in Figure 4. The crystal faces and axes were identified by optically determining the angle between the (100) and (001) faces. The angle was found to be 80°-21'. The reported value is 80°-00' (27). Further evidence for the location of the b axis was obtained when it was determined that the crystals were easily split

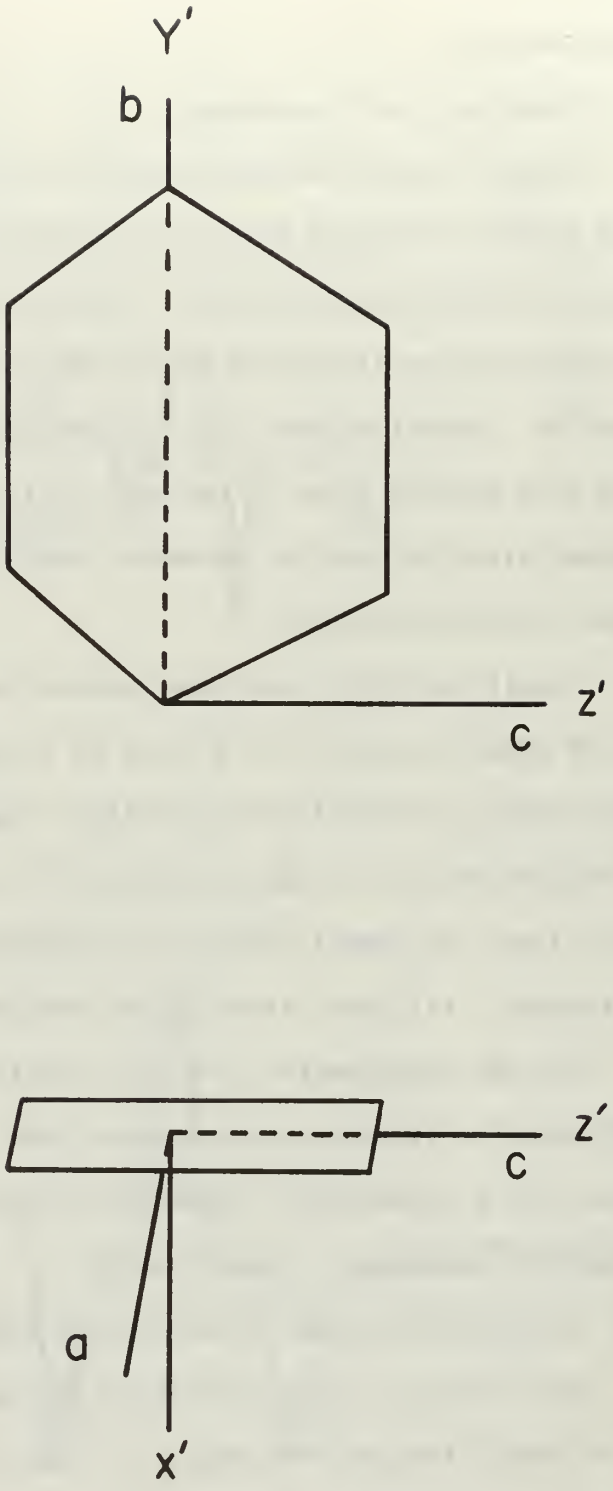

Figure 4. A single crystal of zinc acetate dihydrate shown in two planes. The crystallographic axes a b c and the orthogonal axis system x', y', z' are illustrated. Crystal dimensions have been enlarged by a factor of 10.

along the proposed b axis in agreement with the observations of Schoening, et al (27). Figure 4 also illustrates the locations of the crystallographic axes, a, b, c, and the location of the orthogonal x', y', z' axis system. The latter system will be used as the crystals reference axis system; and henceforth all referrals to the crystals axis system are defined in the x', y', z' system.

4.3 The Initial Polycrystalline Investigation

After being irradiated at 77°K the polycrystalline samples were tapped to the opposite ends of their sealed quartz containers while still emersed in liquid nitrogen so that irradiated portions of the quartz tubing would not enter the spectrometer cavity. The tubing was then quickly transferred to the cavity which had been precooled to 103°K. As a matter of routine investigation, spectra were taken with the sample at various temperatures from 103°K to 300°K. One set of spectra taken at 103°K revealed that a paramagnetic species which is initially produced as a result of irradiation undergoes conversion into another species in a short time. The second species was found to be quite stable at room temperature. Several spectra illustrating the conversion are shown in Figure 5.

Spectra identical to those seen after conversion were observed when polycrystalline samples were irradiated and examined at room temperature immediately after irradiation. This apparently implies that conversion occurs quite rapidly in these samples.

In order to gain further knowledge of the second species, the procedure was reversed and spectra were taken with the sample at various temperatures from 300°K to 103°K. Some of the spectra are shown in

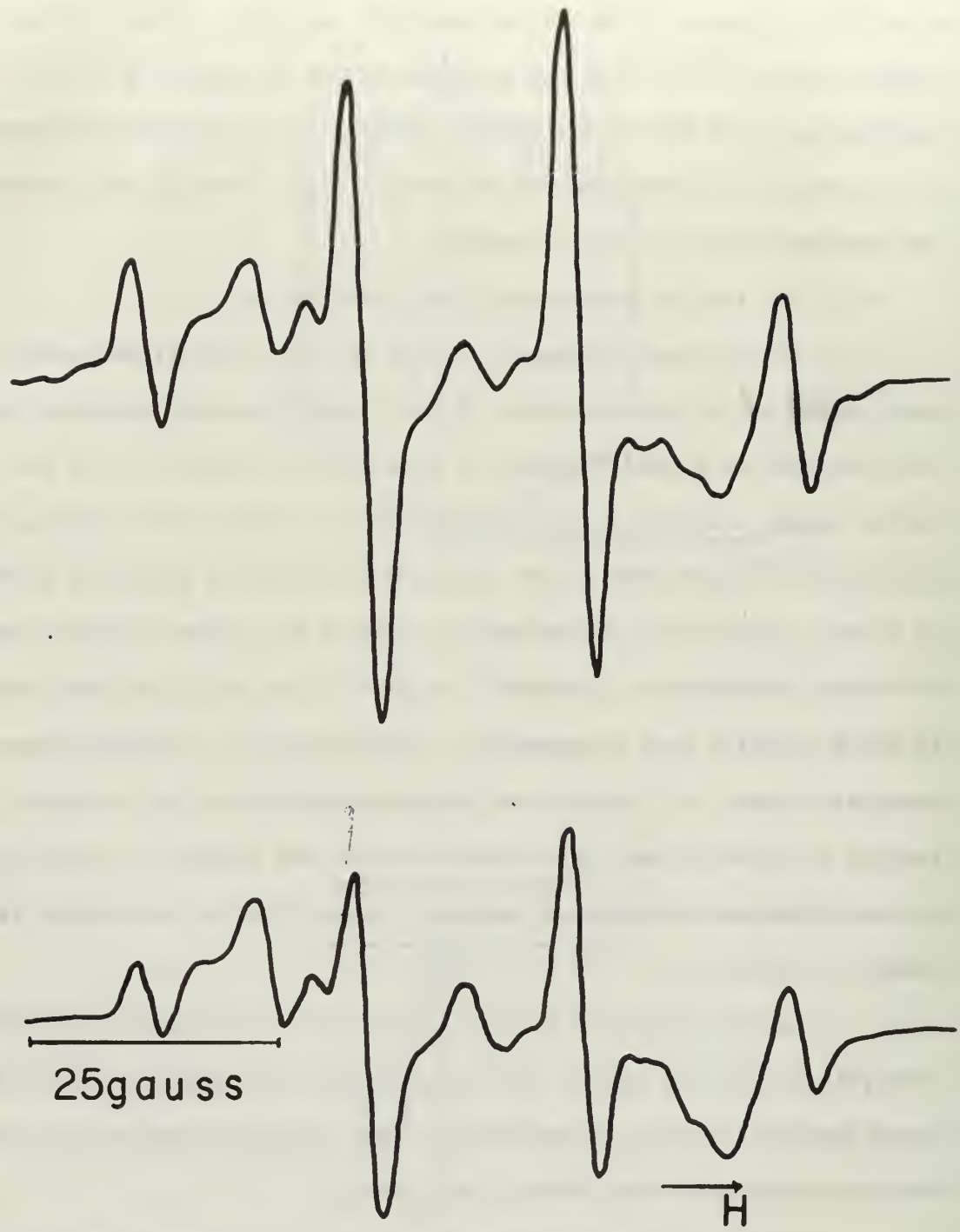

Figure 5. ESR spectra of polycrystalline zinc acetate dihydrate irradiated at 77°K and examined at 103°K at various times. The conversion of one radical species into another is evident.

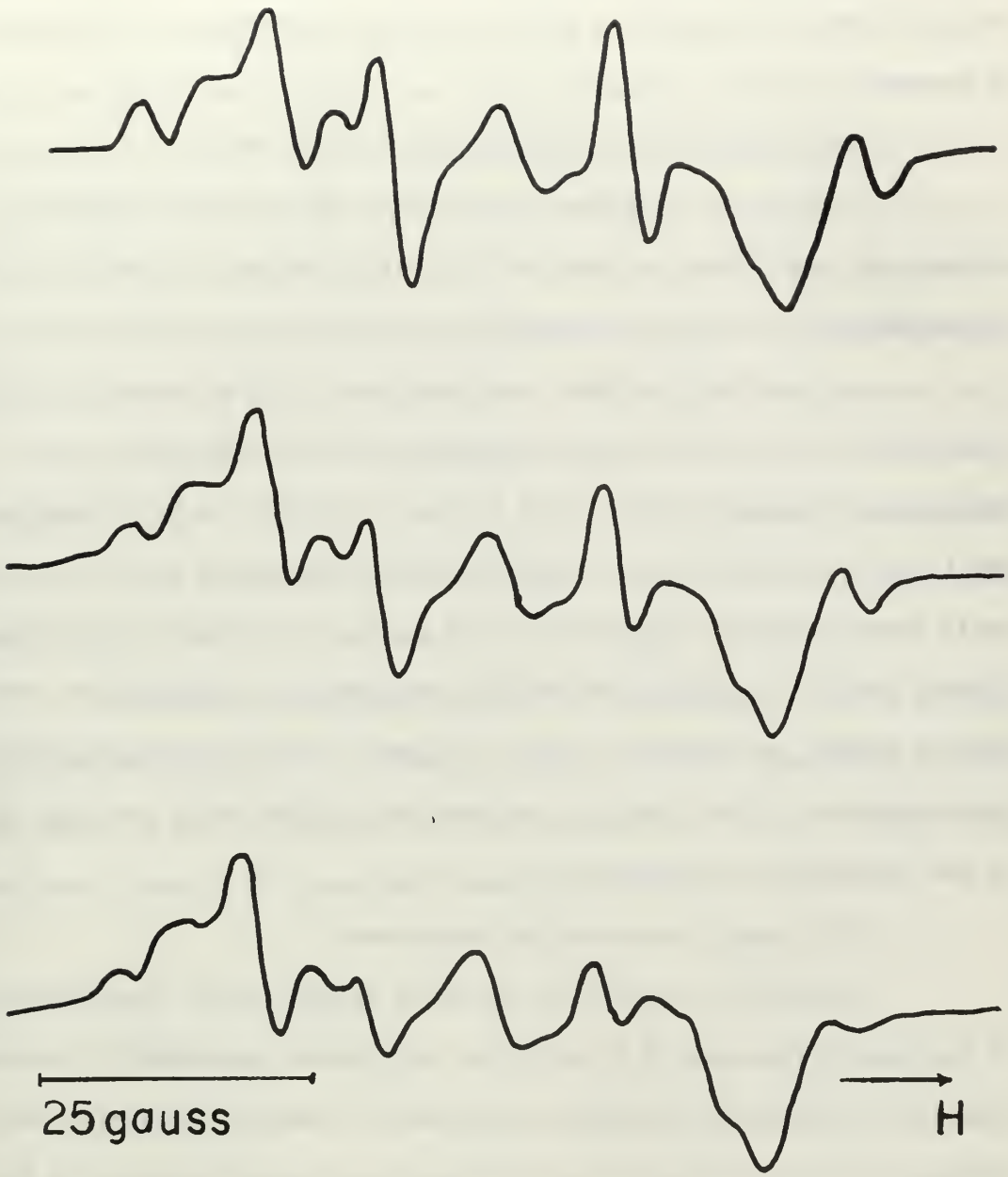
25 gauss
H

Figure 6. A noticeable deterioration of resolution with decreasing temperature is apparent. Nevertheless, it was felt that the spectra revealed that the centerline splits as the temperature of the sample is lowered.

4.4 The Single Crystal Line Splitting Experiment

A study of irradiated single crystals of zinc acetate dihydrate was undertaken in hopes of obtaining further information about the paramagnetic species present after conversion has taken place.

An irradiated crystal was positioned in the magnetic field such that its axis system was coincident with the unprimed x,y,z laboratory reference system. The z axis is defined to be horizontal and in the direction of the magnetic field; the y axis points vertically upward; and the direction of the x axis is defined by the cross product $\vec{y} \times \vec{z}$. Spectral observations were made at temperatures from 20°C to -140°C in intervals of 20°. Figure 7 shows conclusively that the centerline of the initial spectrum does indeed split into two lines as the temperature is decreased.

4.5 The Tensor Determination Experiment

In order to accumulate the data necessary for determination of the tensor elements of $\vec{\vec{g}}$ and $\vec{\vec{A}}$ for the second paramagnetic species observed in the polycrystalline experiment, a series of spectra were obtained for three orientations of irradiated single crystals in the magnetic field. The orientations correspond to rotations about each of the crystals reference axes.

An irradiated crystal was mounted on a flat which had been ground parallel and to the depth of the longitudinal axis of a quartz rod for rotations about the y' and z' axes. The crystal was mounted in such a way that the desired axis of rotation would be parallel to

the longitudinal axis of the rod. An identical flat ground at the opposite end of the rod was optically determined to be parallel to the flat used for mounting to within $\frac{1}{2}^{o}$. The rod was then clipped to an angle indicator positioned so as to be suspended over the center of the spectrometer cavity. It was estimated that the angular position of the crystal could be measured accurately to within $\pm 1^{o}$ by this apparatus. Rotation of the crystal about its x' axis was accomplished as described above with the exception of the mounting procedure. Here the crystal was mounted on the end of a quartz rod. The end had been ground so as to be perpendicular to the longitudinal axis of the rod. An optical measurement implied that the end was within 1^{o} of perpendicularity with the axis. A flat ground into the opposite end of the rod as described above allowed the rod to be coupled to the angle indicator.

The observations were made at a temperature of $133^{o}K$ as both splitting and signal to noise were optimal at this temperature. Spectra were taken at 15^{o} rotational intervals about the y' and z' axes, whereas they were taken at 5^{o} intervals about the x' axis.

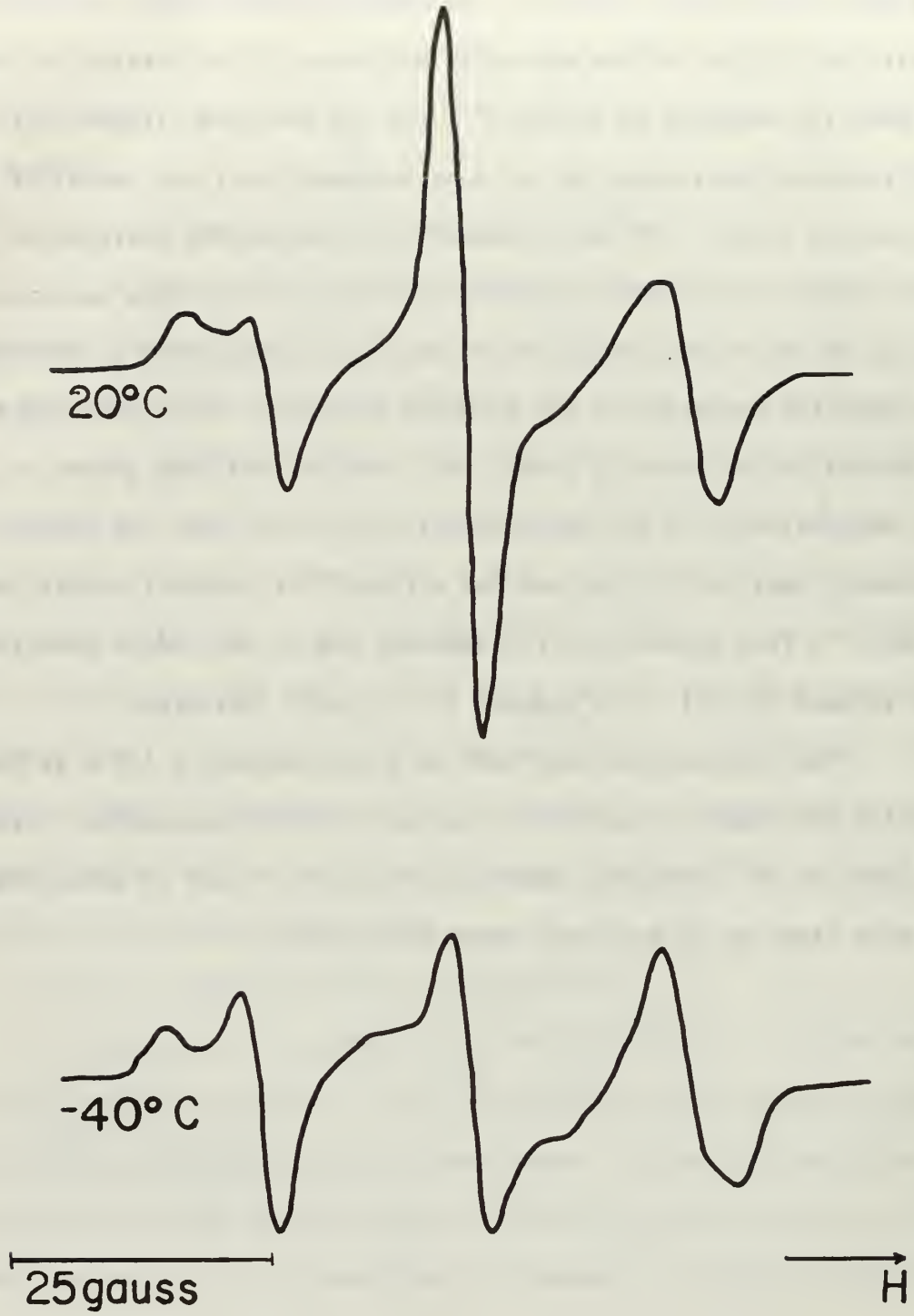

Figure 6. The temperature dependence of the ESR spectrum of the radical present in irradiated polycrystalline zinc acetate dihydrate after conversion has occurred. The splitting of the centerline of the 20°C spectrum as the temperature is lowered is evident.

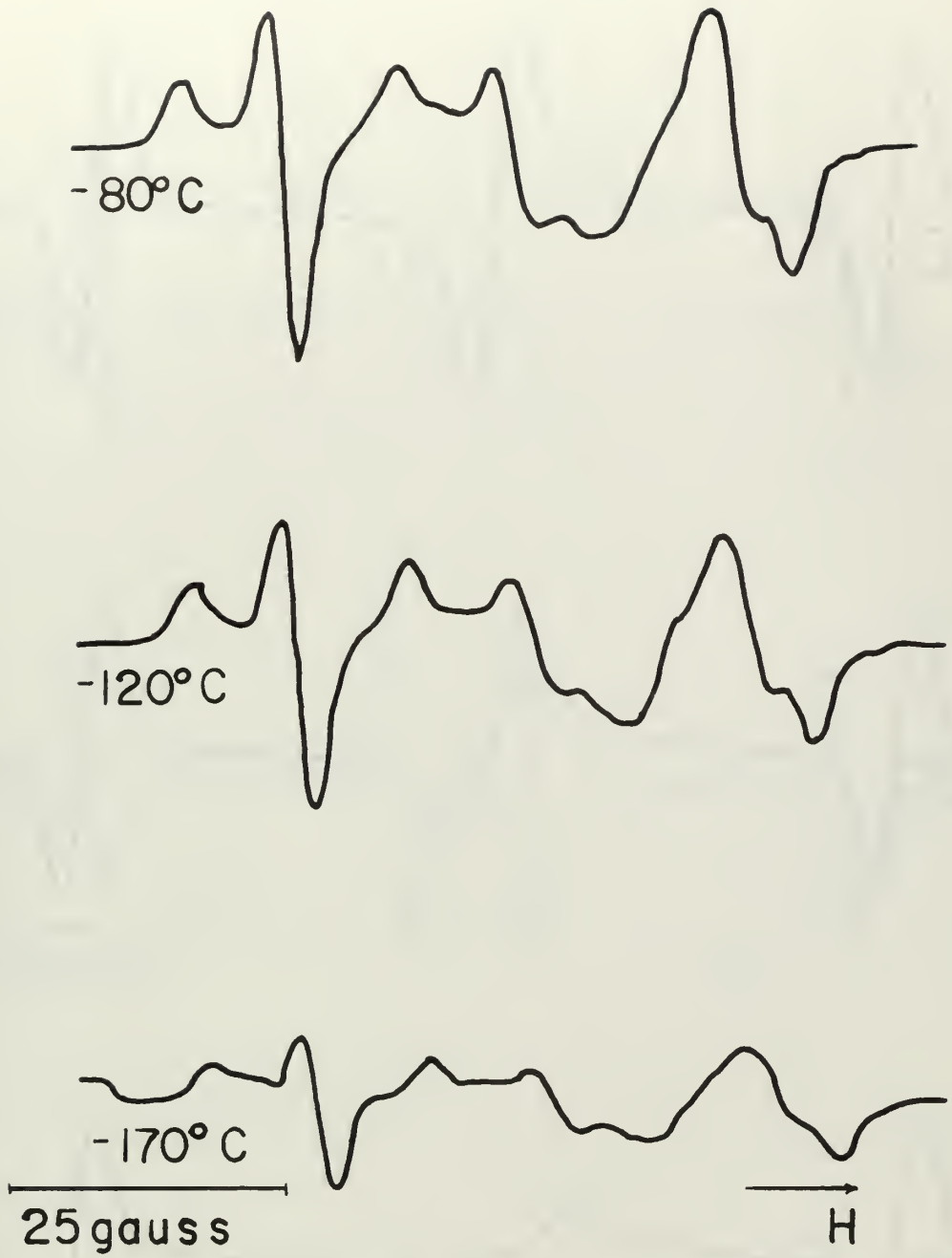
-80° C
-120° C
-170° C
25 gauss
H

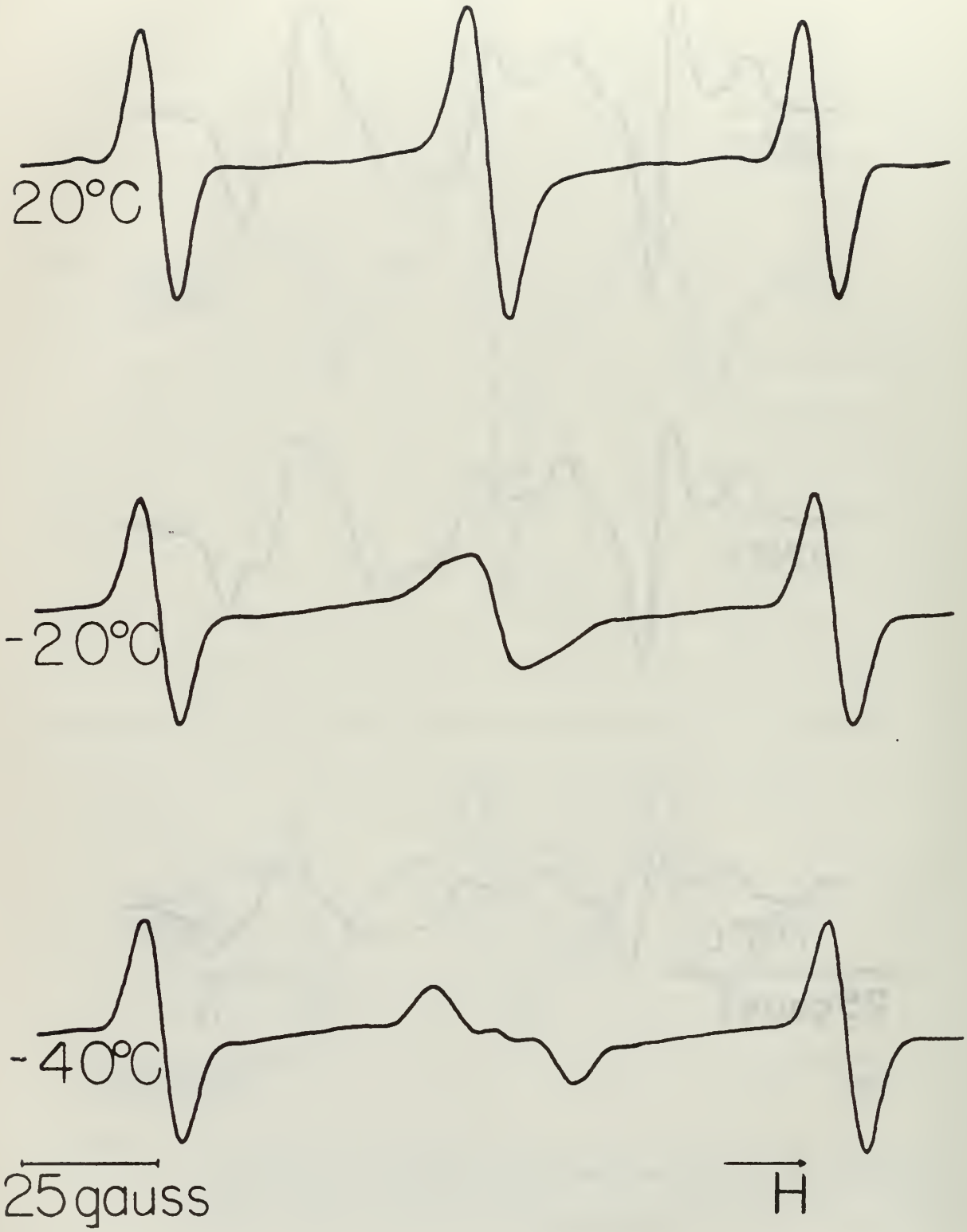

Figure 7. The temperature dependence of the ESR spectrum of the radical present in irradiated single crystals of zinc acetate dihydrate after conversion has occurred. The splitting of the centerline of the 20°C spectrum as the temperature is lowered is most obvious.

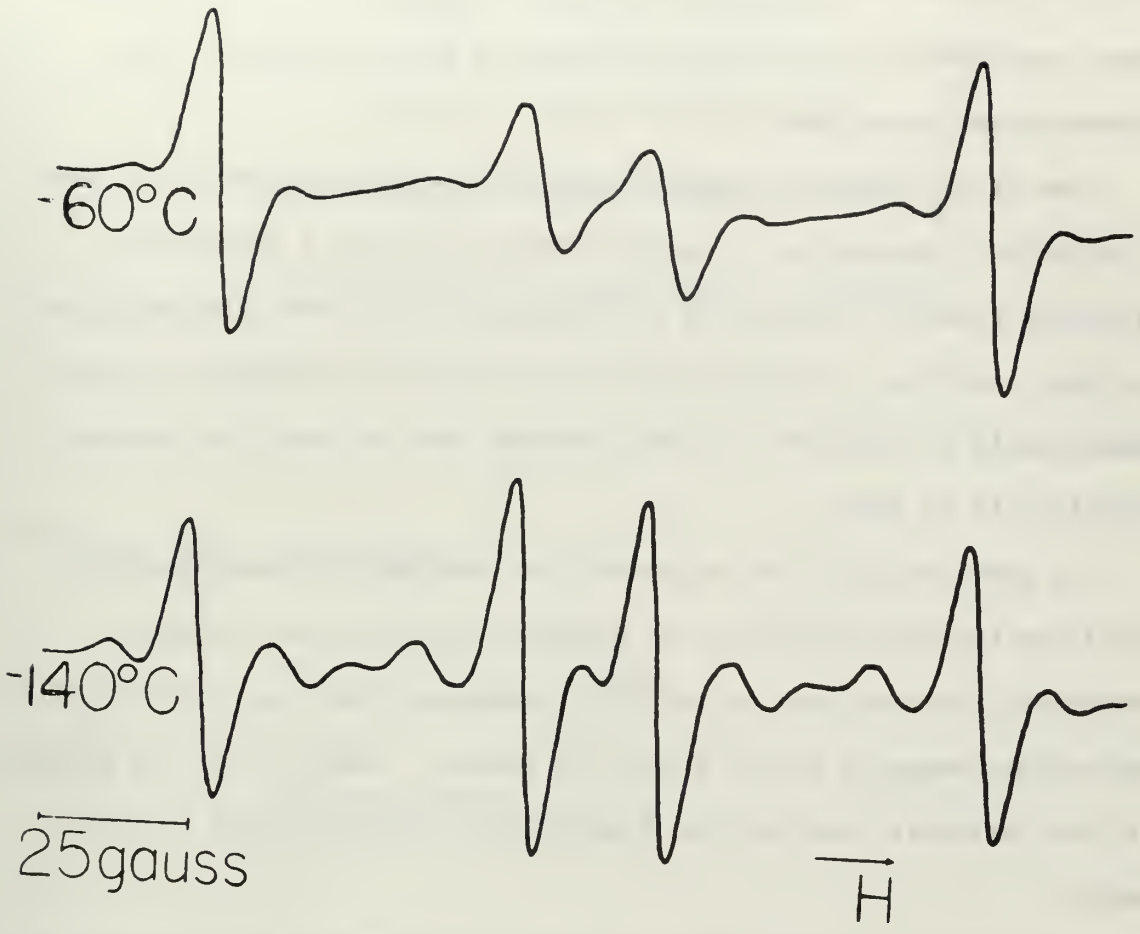
-60°C
-140°C
25gauss
H

5. The Effect of Rate Processes on Line Shapes

An investigation of the literature revealed that rate process phenomena have been observed in magnetic resonance studies (10). Assuming that the process responsible for the splitting observed in the temperature experiment was interatomic exchange a detailed study of the phenomena was undertaken.

One of the simplest examples of these phenomena would be the case of a nuclear spin moving at random between two sites A and B with different chemical shifts. If the exchange rate between the two sites is rapid, one line, characteristic of the average environment of the nucleus,will be observed. If the exchange rate is slow, two separate signals will be seen.

An expression for the expected line shape may be developed by modifying the Bloch equations to include the effects of exchange. Ordinarily the solutions to the Bloch equations give the variation of macroscopic magnetic moment $\vec{M}$ per unit volume. However, for the purposes of this particular application a rotating coordinate system is more useful.

If we express components of nuclear magnetization in the rotating coordinate system, equations for the total magnetization due to the sites A and B may be written as:

$$u = u_A + u_B$$

$$v = v_A + v_B$$

$$M_z = M_z^A + M_z^B$$

where u denotes the components of nuclear magnetization in phase with the effective rotating component of the rf field, v represents those out of phase with the rotating field, and M represents those in the direction of the stationary field (20).

If H_1, the strength of the rotating field, is small (no saturation) $M_z \cong M_o$, its equilibrium value (11) and $\dot{u}$ and $\dot{v}$ may be expressed as:

$$\dot{u}_A + u_A/T_{2A} + \Delta\omega_A v_A - u_B/T_B = 0$$

$$\dot{u}_B + u_B/T_{2B} + \Delta\omega_B v_B - u_A/T_A = 0$$

$$\dot{v}_A + v_A/T_{2A} - \Delta\omega_A u_A - v_B/T_B = -\gamma H_1 M_{oA}$$

$$\dot{v}_B + v_B/T_{2B} - \Delta\omega_B u_B - v_A/T_A = -\gamma H_1 M_{oB}$$

T_{2A} and T_{2B} are defined

$$1/T_{2A} = 1/T_{2A} + 1/T_A$$

and

$$1/T_{2B} = 1/T_{2B} + 1/T_B$$

where T_{2A} and T_{2B} are the transverse relaxation times and T_A and T_B are the first order lifetimes of the nucleus in A and B (20).

If we now define the complex moments G_A and G_B as

$$G = u_A + iv_A$$

$$G_B = u_B + iv_B$$

the following equations for $\dot{G}_A$ and $\dot{G}_B$ may be obtained:

$$\dot{G}_A + {}_A G_A = i\gamma n H_1 M_{oA} + G_B/T_B - G_A/T_A \quad (5\text{-}1)$$

$$\dot{G}_B + {}_B G_B = i\gamma n H_1 M_{oB} + G_A/T_A - G_B/T_B \quad (5\text{-}2)$$

where α_A and α_B are given by the complex quantities

$$\alpha_A = \frac{1}{T_{2A}} - i(\omega_A - \omega)$$

and

$$\alpha_B = 1/T_{2B} - i(\omega_B - \omega) \qquad (25)$$

Equations (5-1) and (5-2) represent the Bloch equations modified to account for exchange between site A and B.

For the case of slow passage $\dot{G}_A = \dot{G}_B = 0$ (25) G the total complex moment is given by

$$G = \frac{i\,\gamma_n H_1 M_o\,(\tau_A + \tau_B) + \tau_A \tau_B(\alpha_A P_B + \alpha_B P_A)}{(1 + \alpha_A \tau_A)(1 + \alpha_B \tau_B) - 1} \qquad (5\text{-}3)$$

where P_A, the probability of the nucleus being at site A, and P_B, the probability of the nucleus being at site B, are defined as

$$P_A = \frac{\tau_A}{\tau_A + \tau_B} \qquad \text{and} \qquad P_B = \frac{\tau_B}{\tau_A + \tau_B}$$

A general expression for the absorption line shape may now be developed by expanding equation (5-3) and retaining only the imaginary portions. The results as reported by Gutowsky and Holm (9) are given by

$$F(\omega) = \frac{\gamma_n H_1 M_o([1 + \tau/T_2]P + \phi R)}{P^2 + R^2} \qquad (5\text{-}4)$$

For the case where the transverse lattice relaxation times T_{2A} and T_{2B} are equal and sites A and B are equally likely locations for the nucleus

$$T_{2A} = T_{2B} = T$$

$$P_A = P_B = \tfrac{1}{2} \qquad \tau_A = \tau_B = 2\tau$$

where $$\tau \equiv \frac{\tau_A \tau_B}{\tau_A + \tau_B}$$

and

$$P = \tau\left[\left(\frac{1}{T_2}\right)^2 - \left[\tfrac{1}{2}(\omega_A + \omega_B) - \omega\right]^2 + \tfrac{1}{4}(\omega_A - \omega_B)^2\right] + \frac{1}{T_2}$$

$$Q = \tau\left[\tfrac{1}{2}(\omega_A + \omega_B) - \omega\right]$$

$$R = \left[\tfrac{1}{2}(\omega_A + \omega_B) - \omega\right]\left[1 + 2\tau/T_2\right]$$

A plot of $dF(\omega)/d\omega$ vs ω was made for various values of τ, half of the lifetime of either site, as shown in Figure 8. It is quite obvious that as τ is increased from an initial value of zero corresponding to coincidence of sites A and B, a splitting similar to that observed in the temperature experiment occurs.

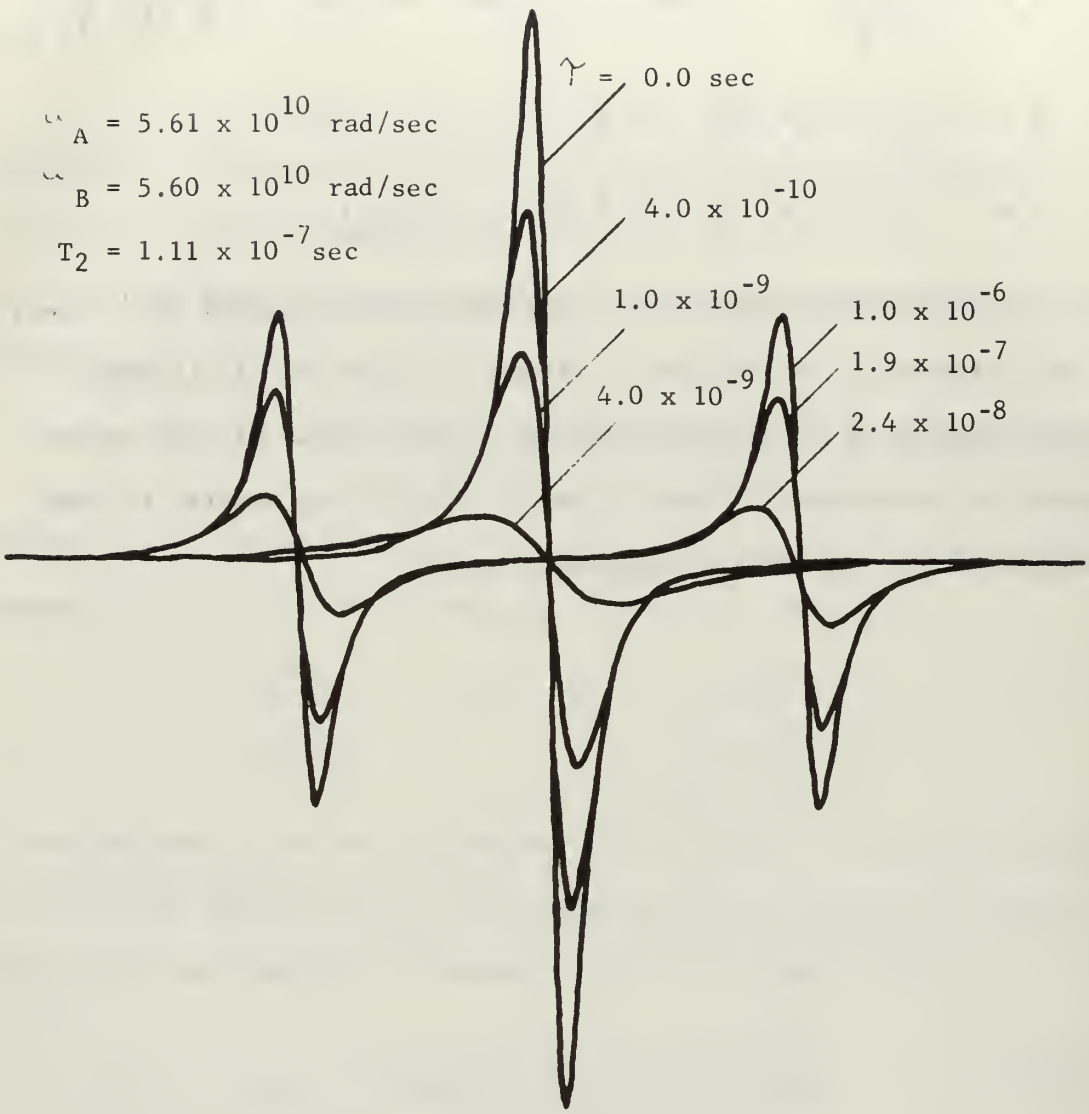

Figure 8. Variations in the first derivative of the shape function $F(\omega)$ with decreasing exchange rate between two positions.

6. Spectrum Interpretation

6.1 The Polycrystalline Spectra

The ESR spectrum of polycrystalline samples irradiated at 77°K and examined at 103°K during the time prior to conversion consists of four lines having relative intensities of 1:3:3:1 and equal splittings of 61.7Mc. An investigation of the literature revealed that the spectrum reported by Kispert and Rogers (14) for the methyl radical in single crystals of sodium acetate trihydrate irradiated and observed at 77°K was quite similar to the experimental spectrum of zinc acetate dihydrate described above. The proton hyperfine splitting reported for the methyl radical was 63.1 Mc (14). The experimental spectrum for zinc acetate dihydrate and a spectrum reproduced from the work of Kispert and Rogers (14) are shown in Figure 9. In view of the excellent agreement of the two spectra the paramagnetic species which undergoes conversion to a second species in polycrystalline zinc acetate dihydrate irradiated at 77°K was identified as the methyl radical.

Because of the availability of single crystals no attempt was made to identify the second species from polycrystalline spectra.

6.2 The Radical $\cdot CH_2CO_2^-$ A Proposed Model

The radical present after conversion in irradiated zinc acetate dihydrate was proposed to be $\cdot CH_2CO_2^-$. Since a study of the $\cdot CH_2CO_2^-H$ radical present in irradiated acetic acid (30) revealed that it has a non-planar structure it was felt that it would be quite logical to assume that the structure of $\cdot CH_2CO_2^-$ would be similar. A non-planar structure having an angle of 120° between the C_2H_1 and C_2H_2 bonds was, therefore, assumed for the model. A sketch of the structure is illustrated in Figure 10. The 4 line room temperature spectrum shown in

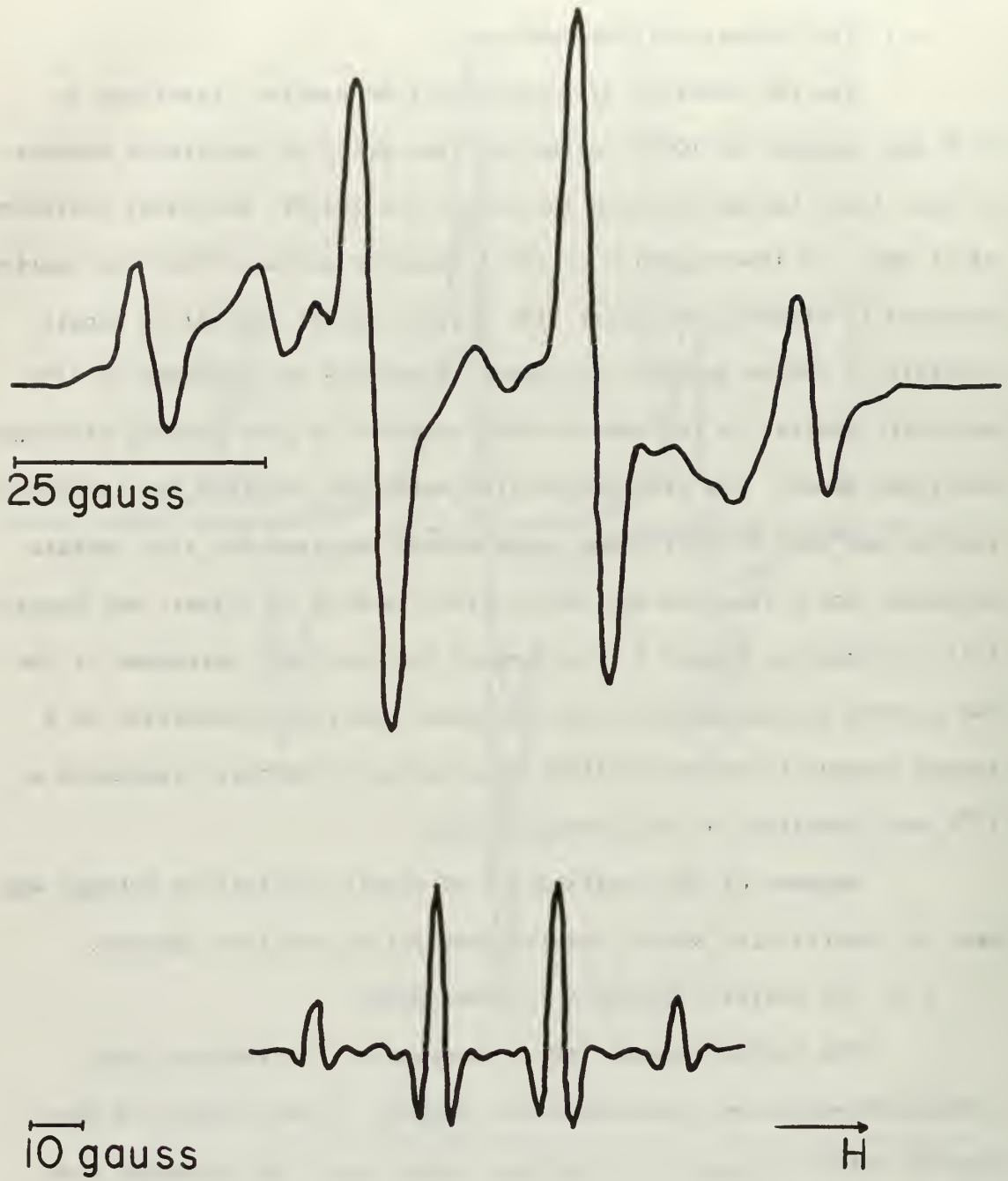

Figure 9. A comparison of the ESR spectrum of polycrystalline zinc acetate dihydrate irradiated at 77°K and examined at 103°K (top) and the ESR spectrum of sodium acetate trihydrate irradiated and examined at 77°K (bottom, reported by Kispert, et al (14)).

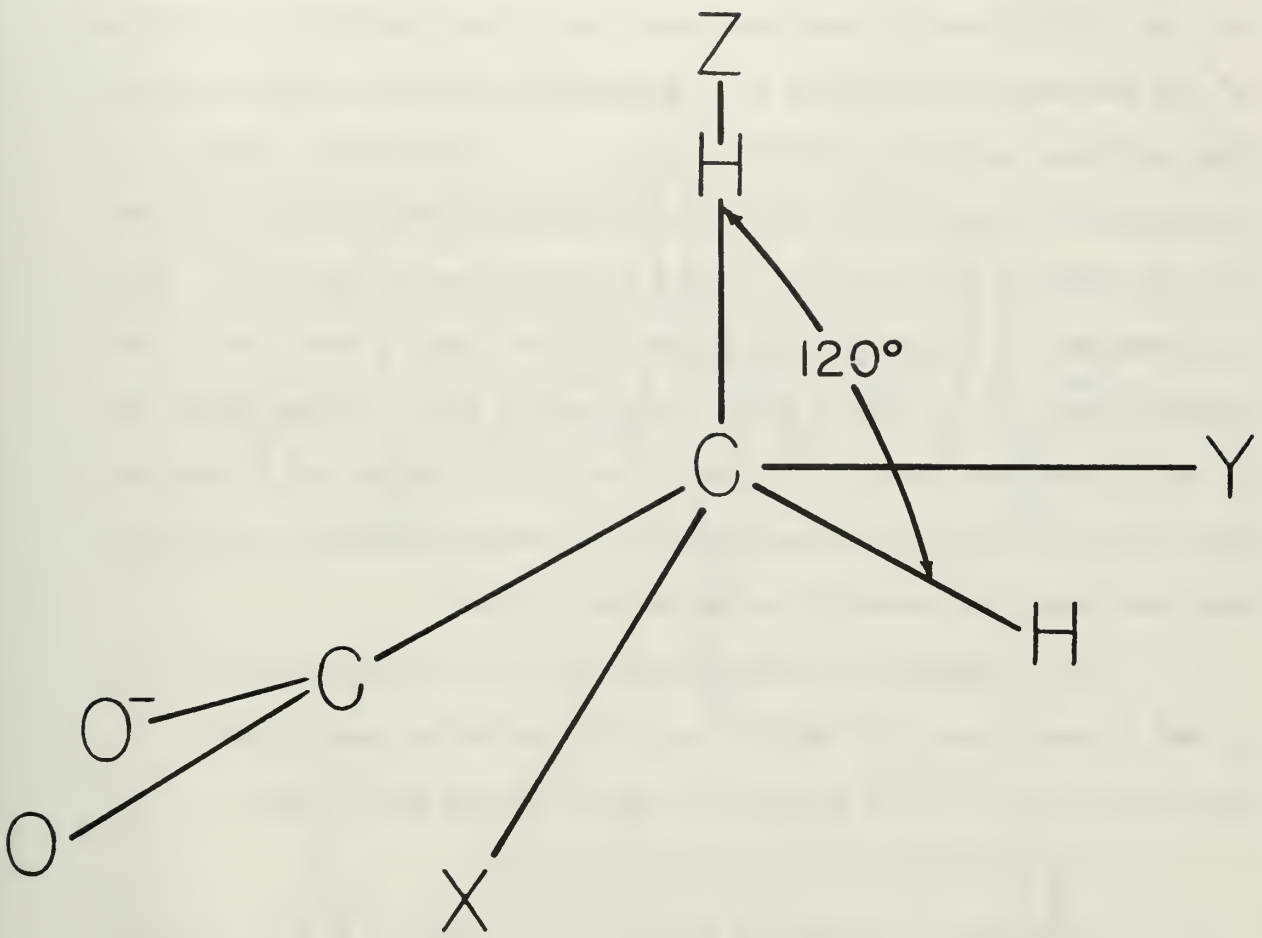

Figure 10. A structural model for $\cdot CH_2CO_2^-$ with the principal axes of H_1 defined. Note that the structure is assumed to be non-planar.

Figure 7 is in accord with that expected from this model; as for all orientations about the y' axis (which is coincident with the two-fold crystallographic axis) the two magnetic sites are equivalent. The line splitting observed in the temperature experiment may be explained as being the result of hindered internal rotation of the two protons about the α-carbon.

The tensor determination experiment provided further evidence for the $\cdot CH_2CO_2^-$ model. Rotations about the y' axis exhibited equivalence of the two magnetic sites for all orientations about the two-fold axis. Some of these spectra are shown in Figure 11. Second order effects of significant intensity were noted when the angle between the y' z' plane and the magnetic field was 45^o. This is also shown in Figure 11. The inequivalence of the sites was apparent in the spectra taken for orientations about the x' and z' axes. Some spectra for rotations about the x' and z' axes are shown in Figures 12 and 13. As predicted by Morton (23), no site splitting (inequivalence) was observed when the two-fold axis was positioned parallel to the magnetic field.

The complexity of the spectra for all orientations about the x' and z' axes between 0^o and 90^o was believed to be significantly increased because of the presence of strong second order lines.

6.3 The Expected α Proton Coupling Tensors

Assuming the positions indicated in Figure 10 for the hydrogen atoms of the α-carbon a principal axis system for the H_1 proton was defined, with the Z axis along the C_2H_1 bond, the X axis perpendicular to Z and in the plane of the C_2H_1 and C_1C_2 bonds and the Y axis mutually perpendicular to X and Z. The principal values for an α proton hyperfine interaction tensor, expressed in the reference system described

Figure 11. ESR spectra of the $\cdot CH_2CO_2^-$ radical from an irradiated single crystal of zinc acetate dihydrate. The magnetic field perpendicular to the two-fold axis and in the x', z' plane.

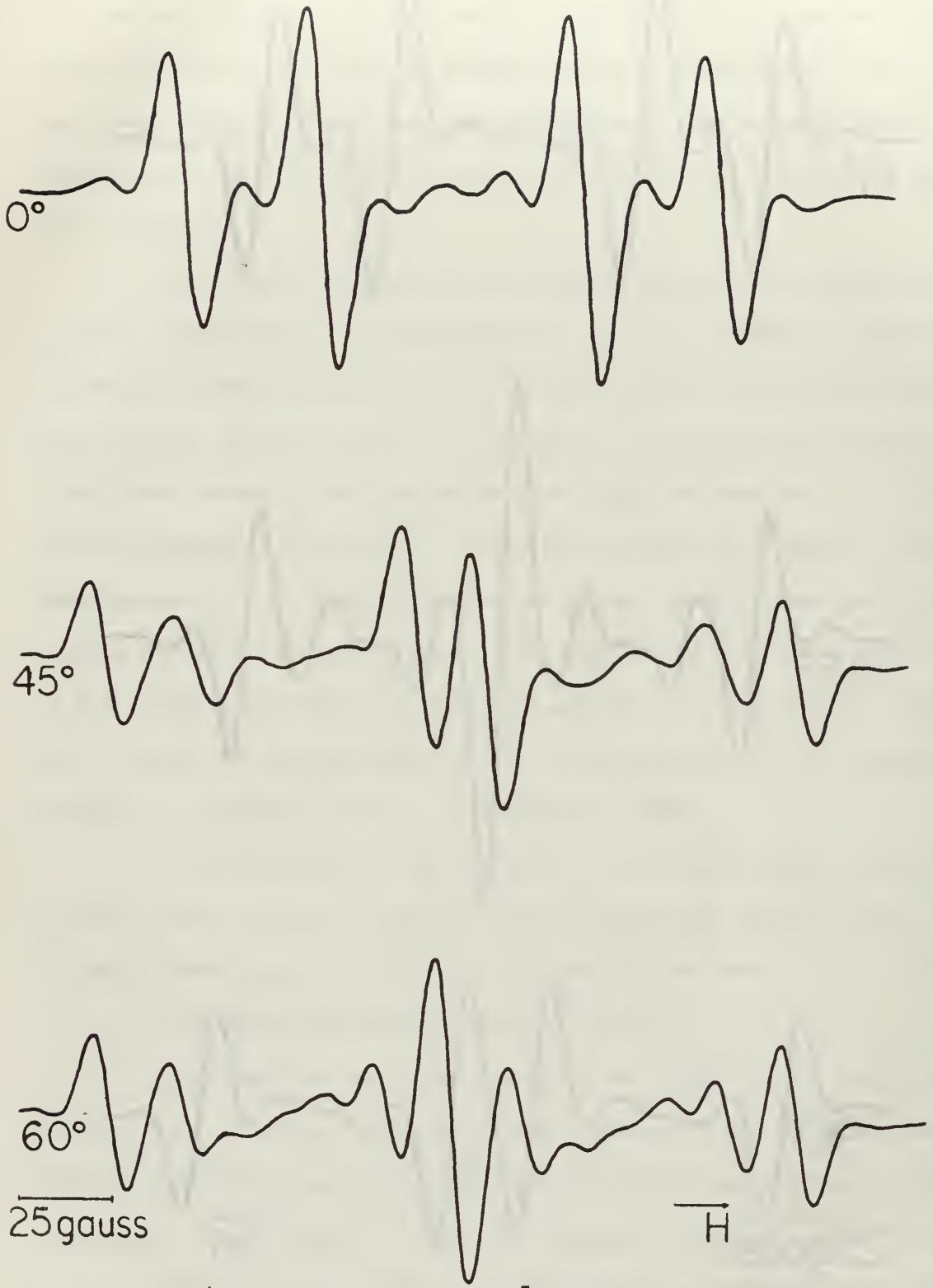

Figure 12. ESR spectra of the $\cdot CH_2CO_2^-$ radical from an irradiated single crystal of zinc acetate dihydrate. The magnetic field perpendicular to the x' axis and in the y' z' plane.

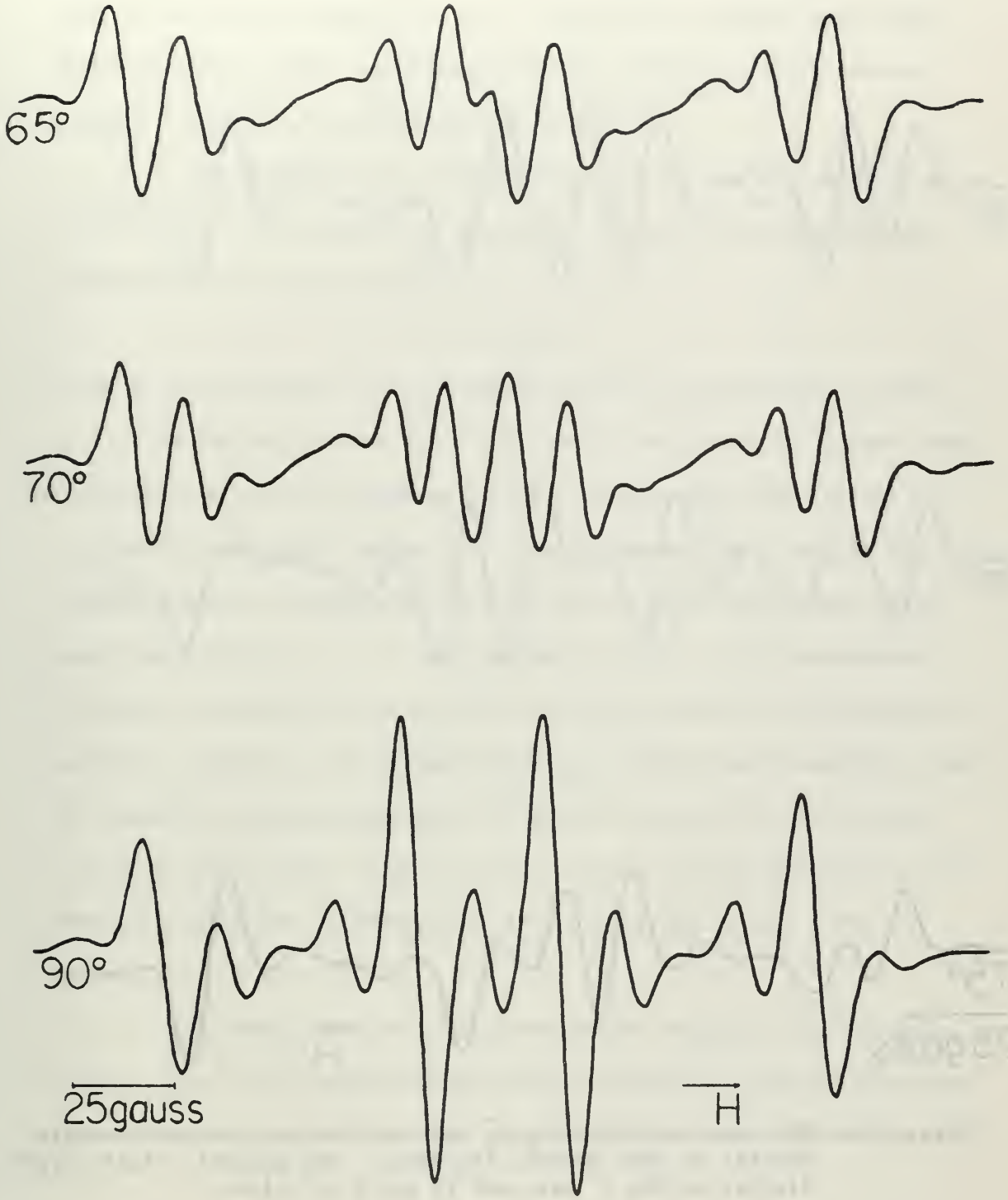
65°
70°
90°
25gauss
H

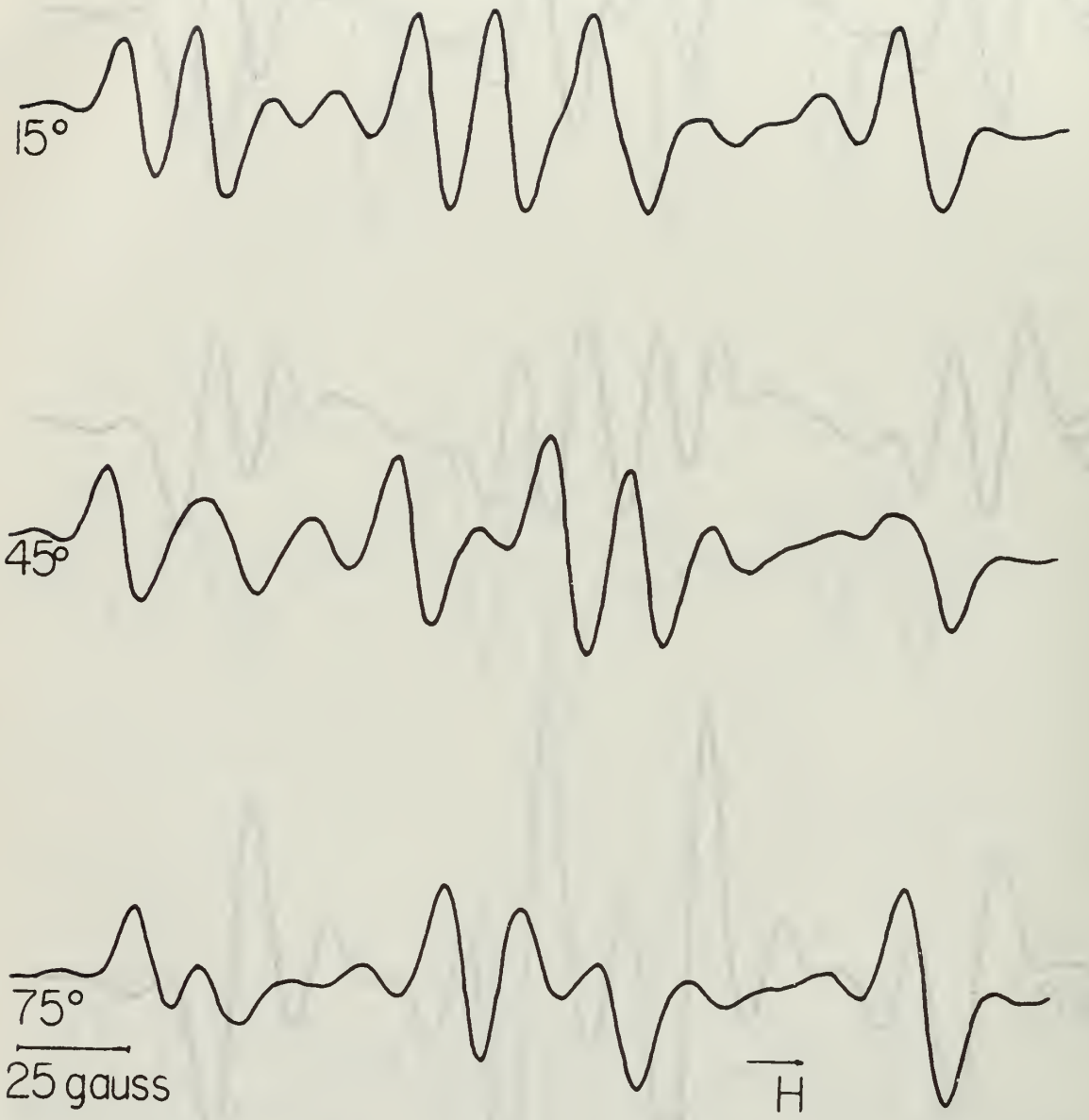

Figure 13. ESR spectra of the $\cdot CH_2CO_2^-$ radical from an irradiated single crystal of zinc acetate dihydrate. The magnetic field perpendicular to the z' axis and in the x' y' plane.

above, have been found to be ; A_{xx} = -91Mc; A_{yy} = -61Mc; and A_{zz} = -29Mc (21). The direction cosines of the X, Y and Z axes with respect to the orthogonal x', y', z' crystal axis system were calculated using the atomic coordinates of one molecule of zinc acetate dihydrate reported by Schoening, et al (27).

The hyperfine interaction tensor of H_1 was then defined in the x', y', z' axis system by performing the matrix multiplications indicated in the expression

$$B = TAT'$$

where A is the matrix of the coupling tensor of H_1 expressed in the X, Y, Z coordinate system; T is the transformation matrix formed from the direction cosines locating the x, y, and z axes with respect to the primed coordinate system; T' is the transpose of T; and B, the resulting matrix, represents the hyperfine interaction tensor of H_1, expressed in the x', y', z' crystal axis system. In a like manner principal axes for H_2 were defined, direction cosines locating these axes with respect to the primed coordinate system were calculated, and the hyperfine interaction tensor of H_2 was expressed in the crystal reference axis system. The direction cosines and the matrices of the resulting hyperfine interaction tensors of H_1 and H_2 are given in Table 1.

Although there are two inequivalent magnetic sites for the acetate ions in the unit cell as shown in Figure 14, the radicals are related by a rotation about the two fold crystal axis. Therefore, the

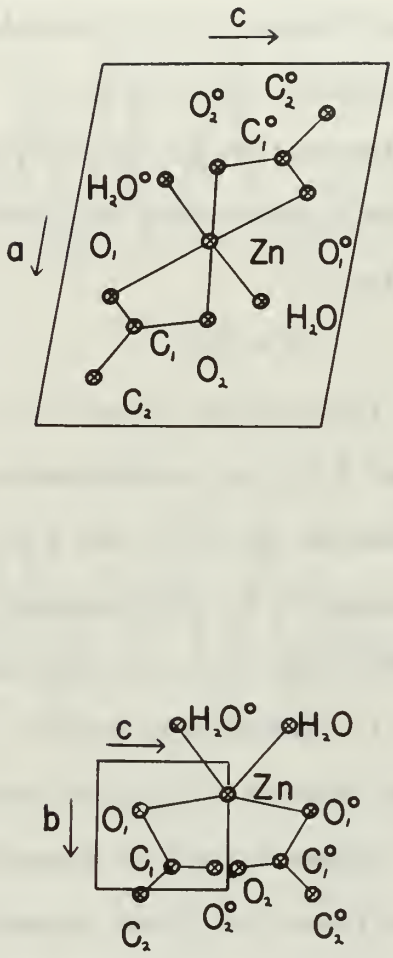

Figure 14. The position of a zinc acetate dihydrate molecule in the unit cell.

hyperfine interaction tensors for the H_1' and H_2' protons of the second molecular site may be determined by transforming the dyadics of H_1 and H_2 through a rotation of 180° about the y' (two-fold) axis. The tensors for H_1' and H_2' are shown in Table 1.

Expressions for the expected line separation for all possible orientations of the crystal in the external magnetic field are readily obtainable. To first order, assuming isotropic g and neglecting the nuclear Zeeman energy the measurable line separations will be the projections of each hyperfine coupling tensor along the magnetic field. These projections may be expressed in terms of the matrix elements shown in Table 1 and trigonometric functions.

The procedure may best be described by developing one of the expressions. Consider the case where the crystal was mounted so that it could be rotated about its x' axis. The locations of the x', y', z' axes with respect to the x, y, z laboratory system (previously defined) are; x' coincides with -y, y' lies along x, and z' is coincident with z. The location of x', y' and z' may be defined with respect to the x, y, z system by the transformation matrix T where

$$T = \begin{pmatrix} 0 & -1 & 0 \\ 1 & 0 & 0 \\ 0 & 0 & 1 \end{pmatrix}$$

If A is defined, for convenience sake, to be the matrix of the hyperfine tensor of H_1 expressed in the primed coordinate system, $\bar{A}$ the matrix representing the hyperfine tensor of H_1 expressed in the laboratory coordinate system can be found by the expression

$$\bar{A} = TAT'$$

where T' is the transpose of T.

Proton	Tensor in x'm y', z' Axis System			Direction Cosines in x', y', z' Axis System
H_1	-35.07	-16.28	3.32	(0.9329,-0.3570,-0.0466)
	-16.28	-73.43	14.36	(0.2564, 0.5678, 0.7822)
	3.32	14.36	-72.51	(0.2528, 0.7417,-0.6213)
H_2	-85.29	-8.23	13.92	(-0.2473,0.8209,-0.5147)
	-8.23	-39.55	-12.87	(0.2561, 0.5677, 0.7824)
	13.92	-12.87	-56.22	(0.9345, 0.0617,-0.3506)
H_1'	-35.07	16.28	3.32	(0.9329, 0.3570,-0.0466)
	16.28	-73.43	-14.36	(0.2564,-0.5678,-0.7822)
	3.32	-14.36	-72.51	(-0.2528,0.7417, 0.6213)
H_2'	-85.29	8.23	13.92	(-0.2473,-0.8209,-0.5147)
	8.23	-39.55	12.87	(-0.2561, 0.5677,-0.7824)
	13.92	12.87	-56.22	(0.9345,-0.0617, 0.3506)

Table 1. Coupling tensors (Mc/s) of the four inequivalent protons present in a unit cell of irradiated zinc acetate dihydrate. (Expected from crystal structure)

Substituting

$$\bar{A} = \begin{pmatrix} 0 & -1 & 0 \\ 1 & 0 & 0 \\ 0 & 0 & 1 \end{pmatrix} \begin{pmatrix} a_{11} & a_{12} & a_{13} \\ a_{21} & a_{22} & a_{23} \\ a_{31} & a_{32} & a_{33} \end{pmatrix} \begin{pmatrix} 0 & 1 & 0 \\ -1 & 0 & 0 \\ 0 & 0 & 1 \end{pmatrix}$$

$$\bar{A} = \begin{pmatrix} a_{22} & -a_{21} & -a_{23} \\ -a_{12} & a_{11} & a_{13} \\ -a_{32} & a_{31} & a_{33} \end{pmatrix}$$

Now if we consider the general case where the crystal has been rotated about its x' axis by an angle α $\bar{A}$ no longer represents the hyperfine coupling tensor of H_1 in the laboratory system. However, we can easily arrive at a matrix B which does represent the coupling tensor of H_1 in the x, y, z system for all rotations about the x' axis. Recalling that x' is coincident with the y axis the rotation may be considered to be about the y axis. If we therefore describe the positions of the x, y, z axes after rotation with respect to their reference positions by means of the transformation matrix

$$T = \begin{pmatrix} \sin\alpha & 0 & \cos\alpha \\ 0 & 1 & 0 \\ -\sin\alpha & 0 & \cos\alpha \end{pmatrix}$$

we can arrive at B by performing the operations indicated in the expression

$$B = TAT'$$

However, since we are only interested in the projection of B on the z axis, b_{33}, we need only develop an expression for that element. Using the general formula

$$b_{ij} = \sum_{k,l} T_{i,k}\bar{A}_{k,l}T_{j,l}$$

it is easily shown that

$$b_{33} = a_{22}\sin^2\alpha + a_{33}\cos^2\alpha + 2a_{23}\sin\alpha\cos\alpha$$

In a like manner, expressions corresponding to rotation about x', y' and z' axis by an angle α for the four protons of the unit cell may be developed. The results are, respectively,

$$b_{33} = a_{22}\sin^2\alpha + a_{33}\cos^2\alpha \pm 2a_{23}\sin\alpha\cos\alpha$$

$$b_{33} = a_{11}\sin^2\alpha + a_{33}\cos^2\alpha \mp 2a_{13}\sin\alpha\cos\alpha$$

$$b_{33} = a_{11}\sin^2\alpha + a_{22}\cos^2\alpha \pm 2a_{12}\sin\alpha\cos\alpha$$

where the top sign of double signs refers to H_1 and H_2 and the bottom sign corresponds to H_1' and H_2'.

6.3 The Experimental Coupling Tensors

Measurements of the line splittings observed for rotations about the y' (two-fold) crystal axis were trivial since effectively only two coupling tensors exist because of the equivalence of the two magnetic sites. Several of the experimental spectra are shown in Figure 11.

The determination of the line separations for rotations about the z' axis was found to be a most difficult task. It was felt that line broadening, resulting in otherwise nonexistant superpositions, due to the existence of intense second order lines was the major cause of difficulty. The complexity of the spectra encountered is shown in Figure 13.

Spectra were taken at rotation intervals of 5^o about the x' axis in hopes that some of the difficulties encountered in the interpretation of the spectra taken about the z' axis might be avoided. Again, however, determination of measurements was not trivial. Again, complex hyperfine structures were encountered. It was determined that meaningful

measurements were not possible unless the behavior of the center structure for the spectra between 0^{o} and 90^{o} rotation was postulated to be that of two lines converging until at 55^{o} and 60^{o} they are coincident and then splitting into two lines again for subsequent rotations. The consequence of this hypothesis is that several lines must then be identified as second order lines which are of intensity comparable to that of the postulated first order lines. Spectra for various angles of rotation about the x' axis are shown in Figure 12.

7. Results

As previously indicated in Section 6.1, a comparison of the ESR spectrum of the radical present in irradiated zinc acetate dihydrate taken prior to conversion with the spectrum of the methyl radical in single crystals of sodium acetate trihydrate irradiated and examines at 77°K (14) provides strong evidence for the identification of the radical present in zinc acetate dihydrate as the methyl radical. The proton hyperfine splitting in the experimental spectrum was -61.7 Mc. This is in good agreement with the value of -63.1Mc reported by Kispert and Rogers (14).

A polar plot of the experimental and expected hyperfine splitting of $\cdot CH_2CO_2^-$ for rotations about the y' axis is shown in Figure 15. It was determined that the apparent disagreement of the two plots could be removed if the expected line splitting curve was recalculated using tensor matrices which were arrived at by performing a transformation of 90° about the y' axis on the matrices given in Table 1. The resulting agreement between the experimental and expected splitting is illustrated in Figure 16. The necessity of this transformation implies one of three things; either the crystallographic axes x' and z' were incorrectly identified in the macroscopic crystal; the crystallographic axis identification performed by Schoening, et al (27) was in error; or the orientation of the acetate ion is not that in the unperturbed crystal. Since it was determined that the angles between the four adjacent faces in the macroscopic crystal having their common edge parallel to the two-fold axis were found to be in nearly exact agreement (80°-21' vs 80°-00', 100°-11' vs 100°-00', 80°-21' vs 80°-00', 99°-59' vs 100°-90') with those reported and the crystals split easily along the plane identified

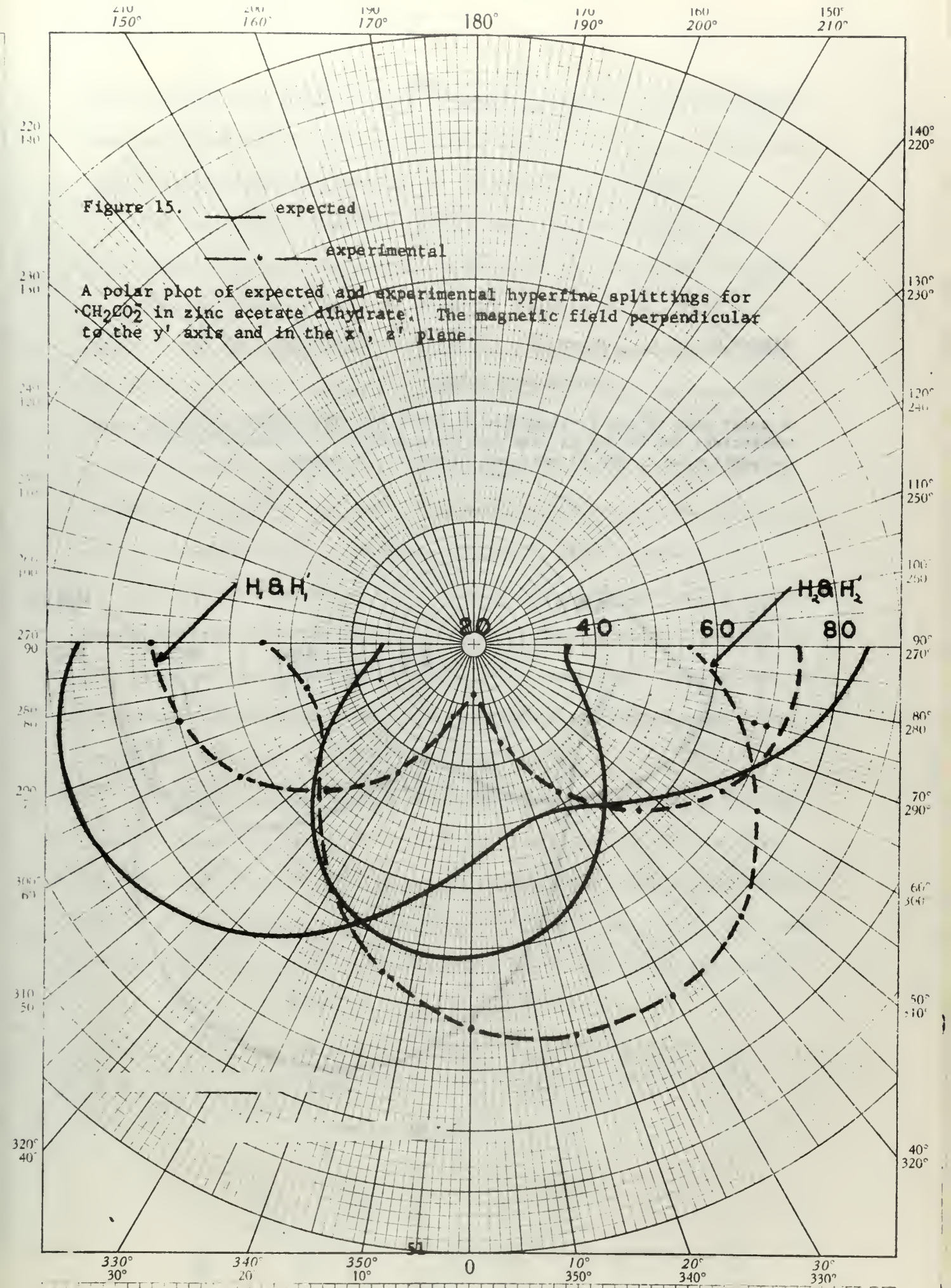

Figure 15. _____ expected

_____ . _____ experimental

A polar plot of expected and experimental hyperfine splittings for $CH_2CO_2^-$ in zinc acetate dihydrate. The magnetic field perpendicular to the y' axis and in the x', z' plane.

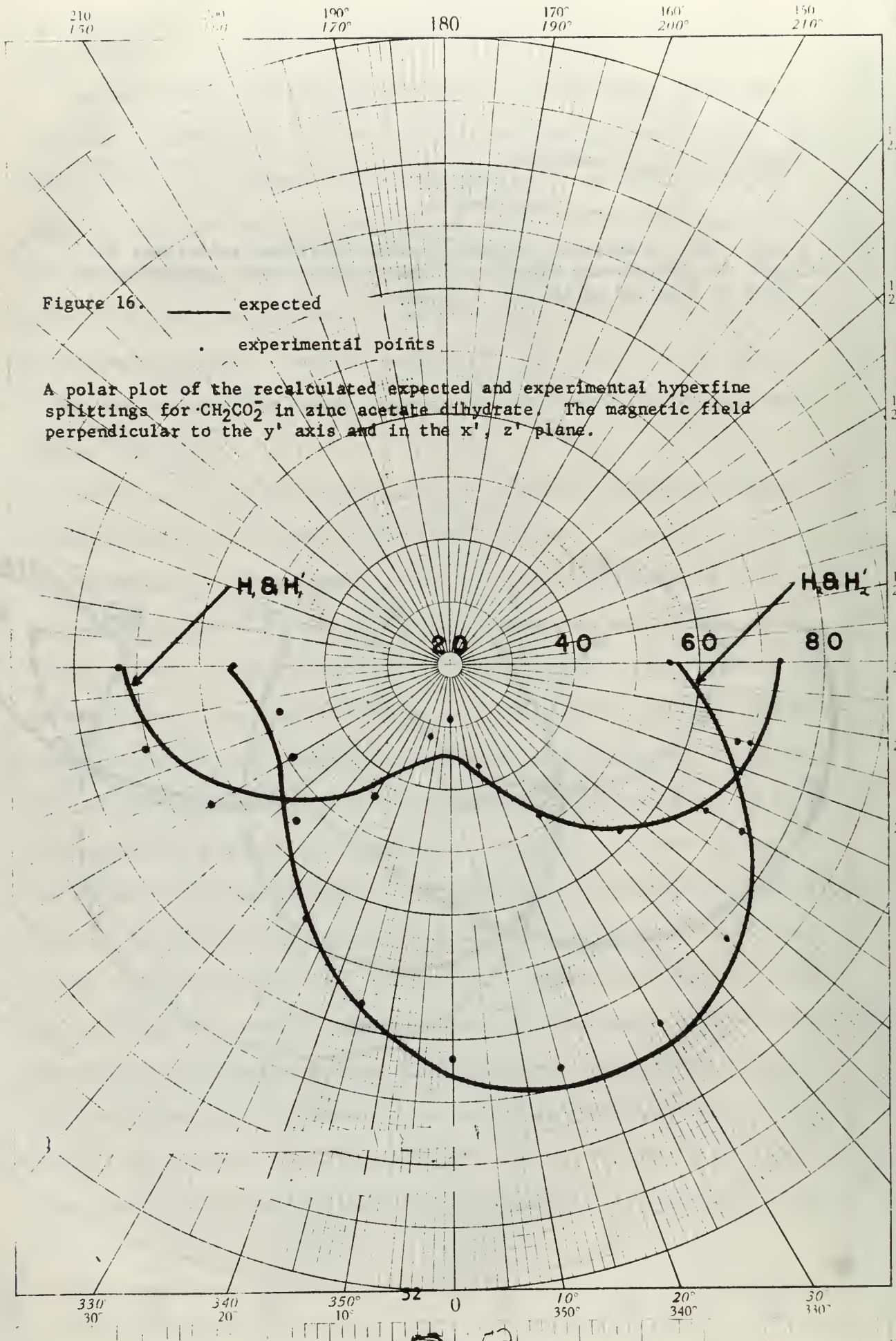

Figure 16. _____ expected

. experimental points

A polar plot of the recalculated expected and experimental hyperfine splittings for $CH_2CO_2^-$ in zinc acetate dihydrate. The magnetic field perpendicular to the y' axis and in the x', z' plane.

as the bc plane as reported (27), it is felt that the crystallographic axes were identified in the macroscopic crystal so as to be consistent with the identification proposed by Schoening, et al (27).

The recalculated coupling tensors and direction cosines of the four inequivalent protons present in the unit cell are shown in Table 2.

Figures 17 and 18 show the expected (calculated as indicated in Section 6.3) and experimental hyperfine splitting for rotations about the x' and z' axes respectively. In both cases a basic agreement between expected and experimental data is apparent. Those areas where agreement between expected and experimental splitting is poor may be considered to result from the presence of strong second order lines in the experimental spectra for those particular orientations.

The matrix elements of the experimental hyperfine coupling tensors were calculated from the experimental line separations with the aid of the formulae developed in Section 6.2. The tensors and their direction cosines are given in Table 3. The estimated experimental error in the principal values of the coupling tensors is $\pm$ 5Mc.

The angle between the C_2H_1 and C_2H_2 bonds was calculated from the two bond eigenvectors, (0.0173, 0.2859, 0.9581) and (0.5843, -0.7211, -0.3722), to be $123.5^{\circ} \pm 5^{\circ}$ where the experimental error was estimated. The value is within the experimental error of the angle 120° which would be expected if strict sp^2 hybridization of the α- carbon exists (11).

Proton	Tensor in x', y', z' Axis System			Direction Cosines in x', y' z' Axis System
H_1	-72.51	14.36	-3.32	(0.0466, 0.3570, 0.9329)
	14.36	-73.43	16.28	(0.7822, 0.5678,-0.2564)
	-3.32	16.28	-35.07	(-0.6213, 0.7417,-0.2528)
H_2	-56.22	-12.87	-13.92	(-0.5147, 0.8209, 0.2473)
	-12.87	-39.55	8.23	(0.7824, 0.5678,-0.2560)
	-13.92	8.23	-85.29	(0.3506,-0.0617, 0.9345)
H_1'	-72.61	-14.36	-3.32	(0.0466,-0.3570, 0.9329)
	-14.36	-73.43	-16.28	(0.7822,-0.5678,-0.2569)
	-3.32	-16.28	-35.07	(0.6213, 0.7417, 0.2528)
H_2'	-56.22	12.87	-13.92	(0.5147, 0.8209,-0.2473)
	12.87	-39.55	-8.23	(0.7824,-0.5677,-0.2561)
	-13.92	-8.23	-85.29	(0.3506, 0.0617, 0.9345)

Table 2. The revised expected coupling tensors of $\cdot CH_2CO_2^-$.

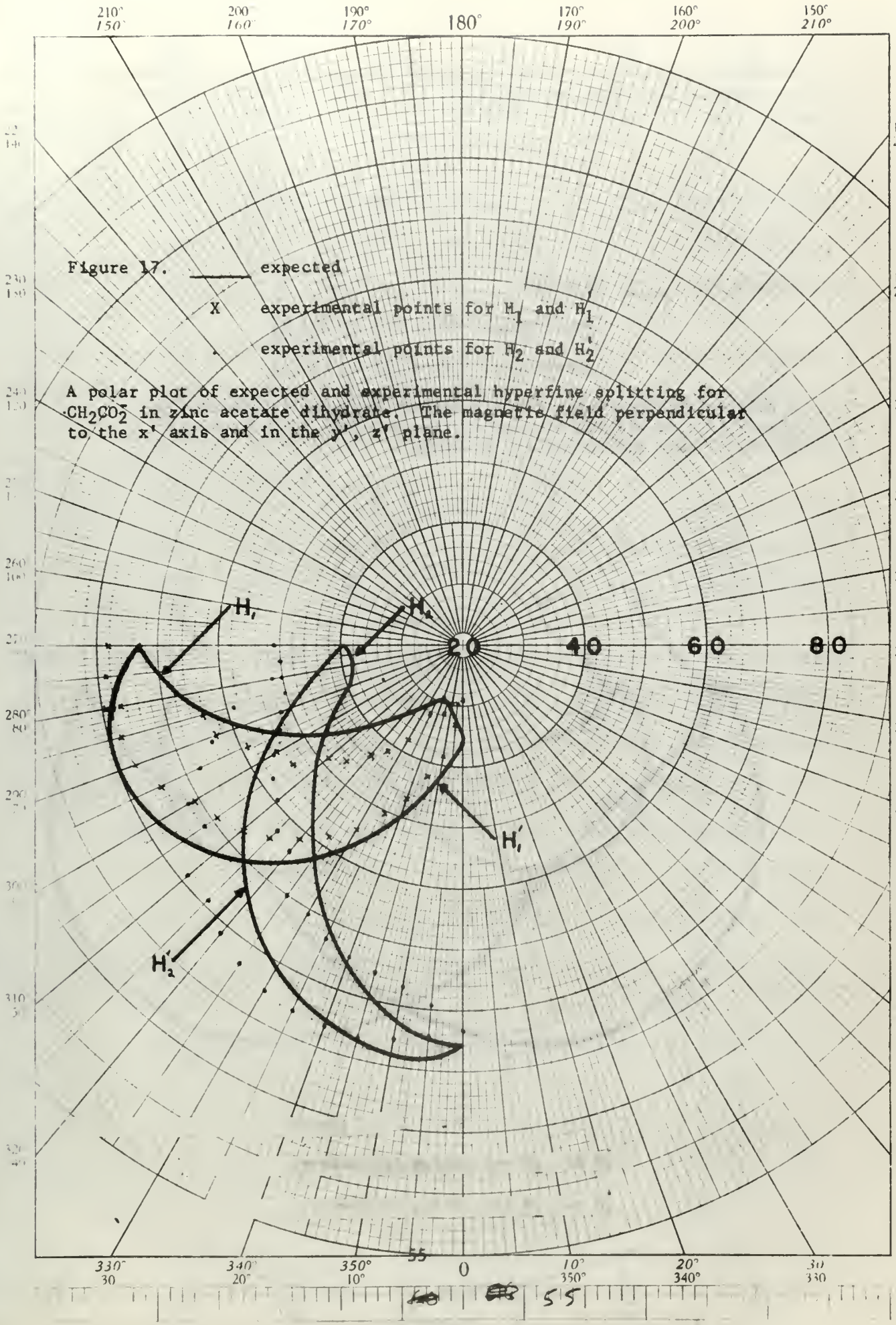

Figure 17. _____ expected

X experimental points for H_1 and H_1'

. experimental points for H_2 and H_2'

A polar plot of expected and experimental hyperfine splitting for $CH_2CO_2^-$ in zinc acetate dihydrate. The magnetic field perpendicular to the x' axis and in the y', z' plane.

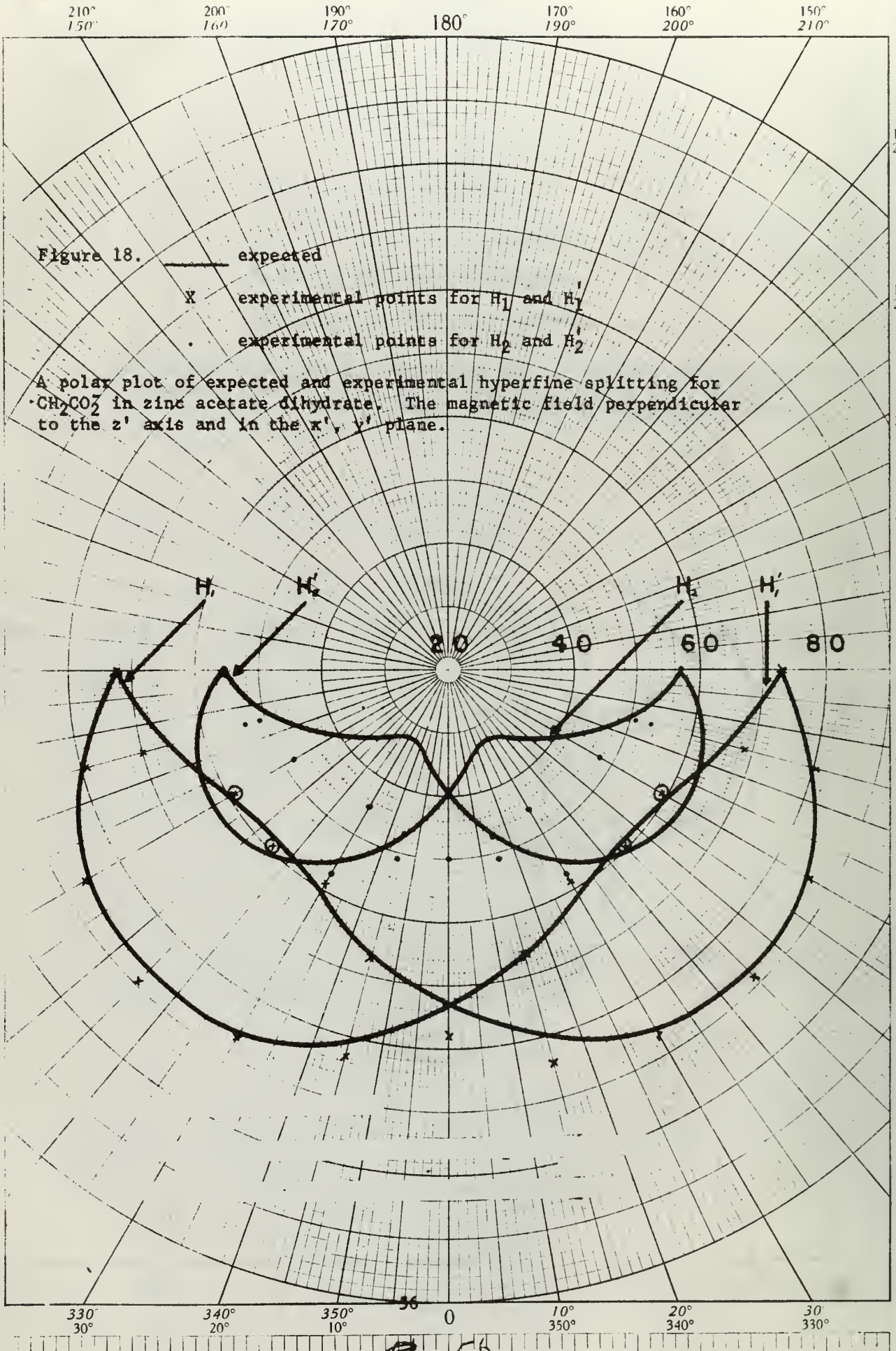

Figure 18. _____ expected

X experimental points for H_1 and H_1'

. experimental points for H_2 and H_2'

A polar plot of expected and experimental hyperfine splitting for $\cdot CH_2CO_2^-$ in zinc acetate dihydrate. The magnetic field perpendicular to the z' axis and in the x', y' plane.

Proton	Tensor in x', y', z' Axis System			Principal Values	Direction Cosines in x', y', z' Axis System
H_1	-73.02	12.44	-2.83	-92 ± 5	(0.0173, 0.2859, 0.9581)
	12.44	-78.32	15.98	-64 ± 5	(0.8261, 0.5358,-0.1748)
	- 2.83	15.98	-28.74	-24 ± 5	(-0.5633,0.7945,-0.02269)
H_2	-55.45	-7.27	-13.32	-91 ± 5	(0.5843,-0.7211,-0.3722)
	-7.27	-50.35	12.53	-60 ± 5	(0.7534, 0.6525,-0.0814)
	-13.32	12.53	-83.17	-38 ± 5	(0.3016,-0.2329, 0.9246)
H_1'	-73.02	-12.44	-2.83	-24 ± 5	(0.0173,-0.2859, 0.9581)
	-12.44	-78.32	-15.98	-64 ± 5	(0.8261,-0.5358,-0.1748)
	-2.83	-15.98	-28.74	-92 ± 5	(0.5633, 0.7945, 0.2269)
H_2'	-55.45	-7.27	-13.32	-38 ± 5	(0.5843, 0.7211,-0.3723)
	7.27	-50.35	-12.53	-60 ± 6	(-0.7534,0.6525, 0.0814)
	-13.32	-12.53	-83.17	-91 ± 5	(0.3016, 0.2329, 0.9246)

Table 3. The experimental coupling tensors (Mc/s) of $\cdot CH_2CO_2^-$.

8. Conclusions

A general computer program for predicting the ESR spectra of polyoriented free radicals has been investigated. Although limited success was achieved it is felt that further modifications of the method used to approximate the spin Hamiltonian could raise the proficiency of the program to an acceptable level. The continuance of the development of this program is justified in that in its present form it offers approximately a 5-fold reduction in computation time as compared to the program reported by Lefebvre and Maruauni (19).

The identification of the methyl radical made by Kitaoka, et al (15) as the paramagnetic species initially created when zinc acetate dihydrate is irradiated has been verified. In addition, the apparent conversion of this radical into another paramagnetic species has been observed. The tentative identification of $\cdot CH_2CO_2^-$ as the long lived free radical formed in irradiated zinc acetate dihydrate after conversion has been substantiated by several means. The splitting of the centerline of the room temperature spectrum with decreasing temperature is considered to result from hindered internal rotation of the two hydrogen atoms about the α- carbon. This phenomena was found to be analogous to other rate processes which have been previously observed in magnetic resonance spectra (9). The low temperature spectra observed for rotations about the y' (two-fold) axis were found to be in agreement with those expected for the $\cdot CH_2CO_2^-$ radical positioned at two magnetically inequivalent sites in the unit cell for all orientations. Similarly, the low temperature spectra for rotations about the x' and z' axes were consistent with the model. Calculated hyperfine interaction tensors for the four inequivalent

protons of the unit cell were found to be in basic agreement with those determined from experimental measurements. However, agreement would not have been attained without assuming the presence of intense second order lines in several of the spectra.

The validity of the proposed identification of certain spectral lines as second order may be checked by performing a calculation to determine a rigorous solution of the spin Hamiltonian. Such a calculation will be carried out in the near future.

Further evidence for the identification of the radical present in zinc acetate dihydrate after conversion may be obtained by performing the tensor determination experiment with single crystals grown from solutions of $Zn(^{13}CH_3COO)_2 \cdot 2H_2O$ and $Zn(CH_3^{13}COO)_2 \cdot 2H_2O$. The presence of additional hyperfine structure in the resulting spectra and the identification of this structure as that expected for the interaction of the unpaired electron with the nuclear spin ($I = \frac{1}{2}$) of the α- carbon (for $Zn(^{13}CH_3COO)_2 \cdot 2H_2O$) and the carboxyl carbon (for $Zn(CH_3^{13}COO)_2 \cdot 2H_2O$) would certainly bolster the evidence for the model.

In view of the results of this experiment it is felt that further x-ray examination of the structural features of zinc acetate dihydrate is justified in that the results of this study imply that the a and c crystallographic axes as defined by Schoening, et al (27) are in actuality interchanged.

Finally, the presence of another paramagnetic species in irradiated zinc acetate dihydrate is suspected. The species is relatively short lived and becomes essentially non-existent approximately twelve hours after irradiation at room temperature. The identification of this species may be very difficult as its spectrum is masked by that of the long lived species $\cdot CH_2CO_2^-$. No attempt was made to identify this species.

BIBLIOGRAPHY

1. Abragam, A., and Pryce, M. H. L., Proc. Roy. Soc. (London) 205, 135 (1951).

2. Adrian, F. J., Bowers, V. A., and Cochran, E. L., J. Chem. Phys., 34, 1161 (1961).

3. Bürk, G., and Schoffa, G., Phys. Status Solidi, 8, 557 (1965).

4. Carrington, A., Ann. Rpts. Chem. Soc., 1964, 27.

5. Carrington, A., and McLachlan, A. D., Introduction to Magnetic Resonance; Harper and Row, Inc., (1967).

6. Cole, T., J. Chem. Phys., 35, 1169 (1961).

7. Cole, T., Fessenden, R. W., Heller, C. and McConnell, H. M., J. Am. Chem. Soc. 82, 776 (1960).

8. Gladney, H. M., and Swalen, J. D., IBM Journal, 515, Nov. (1964).

9. Gutowsky, H. S., and Holm, C. H., J. Chem. Phys., 25, 1228 (1956).

10. Gutowsky, H. S., McCall, D. W., and Slichter, C. P., J. Chem. Phys., 21, 279 (1953).

11. Horsfield, A., Morton, J. R., and Whiffen, D. H., Mol. Phys. 4, 327 (1961).

12. Jones, M. T., and Phillips, W. D., Ann. Rev. Phys. Chem., 17, 323 (1966).

13. Kasai, P. H., and Kirshenbaum, A. D., J. Am. Chem. Soc., 87, 3069 (1965).

14. Kispert, L. D., and Rogers, M. T., J. Chem. Phys., 46, 221 (1967).

15. Kitaoka, M., Takeuchi, N., Sasakura, H., and Mizuno, T., Osaka Furistu Kogyo Shoreikan Hokoku, 32, 1 (1964).

16. Kivelson, D., and Neiman, R., J. Chem. Phys., 35, 156 (1961).

17. Kneubühl, F. K., J. Chem. Phys., 33, 1074 (1960).

18. Lefebvre, R., and Maruauni, J., J. Chem. Phys., 42, 1480 (1965).

19. Lefebvre, R., and Maruauni, J., J. Chem. Phys., 42, 1946 (1965).

20. McConnell, H. M., J. Chem. Phys., 28, 430 (1958).

21. McConnell, H. M., Heller, C., Cole, T., and Fessenden, R. W., J. Am. Chem. Soc., 82, 766 (1960).

22. McConnell, H. M. and Robertson, R. E., J. Chem. Phys., 29, 1361 (1958).

23. Morton, J. R., Chem. Rev., 64, 453 (1964).

24. Pake, G. E., Paramagnetic Resonance; W. A. Benjamin, Inc., (1962).

25. Pople, J. A., Schneider, W. G., and Bernstein, H. J., High-resolution Nuclear Magnetic Resonance; McGraw-Hill, Inc., (1959).

26. Sands, R. H., Phys. Rev. 99, 122 (1955).

27. Schoening, F. R. L., Talbot, J. H., and van Niekerk, J. N., Acta Cryst., 6, 720 (1953).

28. Slichter, C. P., Principles of Magnetic Resonance; Harper and Row, Inc., (1963).

29. Tolles, W. M., A Computer Program for Simulation of EPR Spectra for Isotropic g and Hyperfine Coupling Tensors, unpublished.

30. Wood, P. B., Smith, P., Smith, T. C., and Pearson, J. T., J. Chem. Phys., 43, 1535 (1965).

APPENDIX 1

A Computer Program for Calculating $dF(\omega)/d\omega$.

The curves illustrated in Figure 8 were calculated and drawn with the aid of the computer program illustrated in this appendix. The program is written in Fortran for use with the CDC 1604 computer.

```
      PROGRAM LINSHAP
C     THIS PROGRAM WILL CALCULATE THE FIRST DERIVATIVE OF THE LINE SHAPE
C     FUNCTION F(W) FOR THE CASE OF THE LINE SPLITTING OBSERVED AT VAR-
C     IOUS TEMPERATURES FOR IRRADIATED ZINC ACETATE DIHYDRATE AND PLOT
C     A CURVE OF DF(W)/DW VS W.
C     THE SCALE IS SET UP SUCH THAT 100 G ARE COVERED IN 15 INCHES
C     THE PROGRAM PLOTS THE CENTER 9 INCHES OF THE 15 INCH EXPERIMENTAL
C     PLOTS
C     CARD 1 CONTAINS 3 NUMBERS *** TAU,TTWO,MODCURV *** WITH
C     FORMAT (2E10.3,I5)
C              TAU=HALF THE LIFETIME OF A PROTON AT EITHER SITE
C              TTWO=THE TRANSVERSE RELAXATION TIME
C              MODCURV=0 IF ONLY ONE CURVE DESIRED PER PLOT, IF SEVERAL
C              ARE DESIRED, 1=1ST CURVE, 2= ALL INTERMEDIATES, 3= LAST
C     CARD 2 CONTAINS 8 NUMBERS *** NUMPTS, IWIDE, IHIGH, DINCR, OFFSET,
C     HLFHT, XSCALE, YSCALE *** WITH FORMAT (3I5, 3F5.2, 2E10.3)
C              NUMPTS= NUMBER OF POINTS TO BE CALCULATED-USED 900
C              IWIDE= THE ABSCISSA- USED 9
C              IHIGH= THE ORDINATE
C              DINCR= AN INCREMENT-EQUAL TO IWIDE/NUMPTS
C              OFFSET= HOW FAR UP YOU WANT THE CURVE TO BE DISPLACED
C              HLFHT= HALF THE HEIGHT OF THE TAU=0 CURVE
C              XSCALE= 1.00E+00
C              YSCALE= 1.00E+00
C     CARD 3 IS THE TITLE CARD FOR THE GRAPH AND MAY NOT EXCEED 48
C     CHARACTERS
C     TO STACK RUNS - IF MODCURV=0 START HERE WITH CARD 1 FOR NEXT RUN
C     IF MODCURV=1 STACK CARDS 1,2,AND 3 THEN YOU NEED ONLY ONE CARD 1
C     FOR EACH OF THE OTHER CURVES (MODCURV= 2, AND 3) TO BE DRAWN ON THE
C     THE SAME PLOT
      DIMENSION HT(900),ITITLE(12),C(900),DYDX(900),FOMEGA(900)
      DO 1 I=1,12
    1 ITITLE(I) = 0
      ITITLE(1) = 4HJOB
      ITITLE(2) = 8H VALENTI
      ITITLE(3) = 8H     BOX
```

```
      ITITLE(4) = 2H V
      LABEL = 4H
      SWEEP = 9.0*100.0/15.0
      OMEGAMI=(2.0*3.1416*(3235.0-SWEEP/2.0)/356.813)*10.0**9
      OMEGAMA=(2.0*3.1416*(3235.0+SWEEP/2.0)/356.813)*10.0**9
      FOMEGAA =(2.0*3.1416*(3235.0+ (100.0/15.0)*0.641) /356.813)*10.**9
      FOMEGAB =(2.0*3.1416*(3235.0- (100.0/15.0)*0.641) /356.813)*10.**9
      DOMEGA = FOMEGAA - FOMEGAB
      WBAR = 0.5*(FOMEGAA + FOMEGAB)
   10 READ 1000, TAU,TTWO,MODCURV
      IF (MODCURV-1)11,11,12
   11 READ 2000,NUMPTS,IWIDE,IHIGH,DINCR,OFFSET,HLFHT,XSCALE,YSCALE
   12 CONTINUE
      PRINT 300
      PRINT 400, NUMPTS, MODCURV, IWIDE,IHIGH,  OFFSET, XSCALE, YSCALE
      PRINT 100
      PRINT 200, TAU,TTWO,FOMEGAA,FOMEGAB,HLFHT
      FNUMPTS = NUMPTS
      J = NUMPTS - 1
      WINCR=(OMEGAMA-OMEGAMI)/FNUMPTS
      OMEGA = OMEGAMI
      S = (1.0 + TAU/TTWO)
      T = (1.0 + TAU/TTWO)
      DO 2 I = 1, NUMPTS
      FOMEGA(I) = OMEGA
      P = TAU*((1.0/TTWO)**2 - (WBAR- FOMEGA(I))**2 + 0.25*(DOMEGA)**2)
     1+ 1.0/TTWO
      Q = TAU*(WBAR - FOMEGA(I))
      R = (WBAR - FOMEGA(I)) *(1.0 + 2.0*TAU/TTWO)
      HT(I) = (T*P + Q*R)/(P**2 + R**2)
    2 OMEGA = OMEGA + WINCR
      AREA = 0.0
      DO 3 I = 1,J
    3 AREA = WINCR*(HT(I +1) + HT(I))/2.    AREA
      PRINT 500, AREA , DINCR
      DO 4 I = 1,NUMPTS
```

```
    4 HT(I) = (HT(I)/AREA)*10.0
      DYDX(1) = 0.0
      DO 5 I = 1,J
    5 DYDX(I+1) = (HT(I+1) - HT(I))/DINCR
      C(1) = 0.0
      DO 6 I = 1,NUMPTS
    6 C(I 1) = C(I) + DINCR
      IF (MODCURV -1)40,40,50
   40 THREE = ABSF(DYDX(1))
      READ 3000, (ITITLE(I), I = 7,12)
      DO 7 I = 1, NUMPTS
      ONE = ABSF(DYDX(I))
      TWO = ABSF (DYDX(I+1))
      IF(ONE-TWO) 20,7,7
   20 FOUR = TWO
      IF (THREE-FOUR) 30,7,7
   30 THREE = FOUR
    7 CONTINUE
   50 DO 8 I = 1,NUMPTS
    8 DYDX(I) = (DYDX(I)/THREE)*HLFHT + OFFSET
      CALL DRAW (NUMPTS,C,DYDX,MODCURV,0,LABEL,ITITLE,XSCALE,YSCALE,0,0,
     12,2,IWIDE,IHIGH,0,LAST)
      GO TO 10
  100 FORMAT (5H  TAU,10X,5H   T2,10X,5H   WA,10X,5H   WB)
 1000 FORMAT (2E10.3,I5)
 2000 FORMAT (3I5,3F5.2,2E10.3)
  200 FORMAT (1P5E20.8)
  300 FORMAT (///,10H    NUMPTS,5X,10H   MODCURV,5X,10H     IWIDE,5X,10H
     1     IHIGH)
 3000 FORMAT (6A8)
  400 FORMAT (4(I10,5X),1P3E20.8)
  500 FORMAT (///,8H AREA = ,1PE20.8,9H DINCR = ,1PE20.8)
      END
      END
```

INITIAL DISTRIBUTION LIST

		No. Copies
1.	Defense Documentation Center Cameron Station Alexandria, Virginia 22314	20
2.	Library Naval Postgraduate School Monterey, California 93940	2
3.	Commandant (PTP-1) U. S. Coast Guard Headquarters 1300 "E" St. N. W. Washington, D. C. 20226	2
4.	Professor William M. Tolles Department of Material Science & Chemistry Naval Postgraduate School Monterey, California 93940	2
5.	LT Joseph L. Valenti (OMR) U. S. Coast Guard Headquarters 1300 "E" St. N. W. Washington, D. C. 20226	1
6.	Department of Material Science & Chemistry Naval Postgraduate School Monterey, California 93940	3

DOCUMENT CONTROL DATA - R&D

(Security classification of title, body of abstract and indexing annotation must be entered when the overall report is classified)

1. ORIGINATING ACTIVITY (Corporate author)
Naval Postgraduate School
Monterey, California

2a. REPORT SECURITY CLASSIFICATION
UNCLASSIFIED

2b. GROUP

3. REPORT TITLE
ELECTRON SPIN RESONANCE STUDY OF FREE RADICAL FORMATION IN IRRADIATED ZINC ACETATE DIHYDRATE

4. DESCRIPTIVE NOTES (Type of report and inclusive dates)
Thesis

5. AUTHOR(S) (Last name, first name, initial)
Valenti, Joseph L.

6. REPORT DATE	7a. TOTAL NO. OF PAGES	7b. NO. OF REFS
June 1967	66	30

8a. CONTRACT OR GRANT NO.	9a. ORIGINATOR'S REPORT NUMBER(S)
b. PROJECT NO.	
c.	9b. OTHER REPORT NO(S) (Any other numbers that may be assigned this report)
d.	

10. AVAILABILITY/LIMITATION NOTICES
[redacted] document is subject to special export controls and each transmittal to foreign nationals may be made only with prior approval of the Naval Postgraduate School

11. SUPPLEMENTARY NOTES	12. SPONSORING MILITARY ACTIVITY
	Naval Postgraduate School, Monterey

13. ABSTRACT

An electron spin resonance analysis of irradiated zinc acetate dihydrate, $Zn(CH_3COO)_2 2H_2O$ has been made. The methyl radical, $\cdot CH_3$ has been identified in the spectra of polycrystalline samples irradiated at 77°K and examined at 103°K. The proton hyperfine splitting was determined to be -61.7 ± 1.0 Mc. The conversion of $\cdot CH_3$ into a radical tentatively identified as $\cdot CH_2CO_2^-$ was observed. The conversion is believed to occur too rapidly to be observed in spectra of samples irradiated at 300°K. The X, Y, Z components of the hyperfine interaction tensors of the α_1 and α_2 protons of $\cdot CH_2CO_2^-$ have been tentatively determined to be : -92 ± 5, -64 ± 5, -24 ± 5; and -91 ± 5, -60 ± 5, -38 ± 5 Mc respectively. The X,Y,Z orthogonal axis system was formulated with the Z axis along the CH_1 bond and the X axis perpendicular to Z and in the plane of the CH and CC bonds. The tensor elements were calculated from first order perturbation theory although second order lines of significant intensity were observed. The H_1CH_2 angle was found to be 123.5° ± 5°. The limits of error on tensor components and the bond angle were estimated. Orientations of the CH bonds were found to be rotated 90° about the b axis from the location implied by the crystal structure.

14. KEY WORDS	LINK A		LINK B		LINK C	
	ROLE	WT	ROLE	WT	ROLE	WT
ESR						
EPR						
Acetates						
Irradiation Damage						
Polycrystalline Spectral Envelope Calculation						
Electron Paramagnetic Resonance						
Free Radicals						
Zinc Acetate						